

Received October 8, 2020, accepted October 19, 2020, date of publication October 22, 2020, date of current version November 3, 2020.

Digital Object Identifier 10.1109/ACCESS.2020.3033075

A Novel Latency Estimation Algorithm of Motor Evoked Potential Signals

JOŠKO ŠODA¹, (Member, IEEE), MAJA ROGIĆ VIDAKOVIĆ²,
JOSIP LORINCZ³, (Senior Member, IEEE), ANA JERKOVIĆ²,
AND IGOR VUJOVIĆ¹, (Member, IEEE)

¹Signal Processing, Analysis, and Advanced Diagnostics Research and Education Laboratory (SPAADREL), Faculty of Maritime Studies, University of Split, 21000 Split, Croatia

²Laboratory for Human and Experimental Neurophysiology (LAHEN), Department of Neuroscience, School of Medicine, University of Split, 21000 Split, Croatia

³Faculty of Electrical Engineering, Mechanical Engineering and Naval Architecture (FESB), University of Split, 21000 Split, Croatia

Corresponding author: Joško Šoda (jsoda@pfst.hr)

ABSTRACT Evaluation of motor evoked potential (MEP) signals elicited by transcranial magnetic stimulation (TMS) over the motor cortex provide a measure of cortico-motor excitability at the time of stimulation. In the research and clinical medical practice, the MEP latency is a relevant neurophysiological parameter to determine conduction time for neural impulses from the cortex to peripheral muscles. State changes at different levels of signal propagation through the neural tissue can significantly influence MEP latency, based on which different medical diagnoses can be issued. This study aims to present the Squared Hard Threshold Estimator (SHTE), which is a novel and improved algorithm for MEP latency estimation. Analyses presented in the paper were based on the SHTE algorithm, which was efficiently applied to a large number of MEP signals recorded from hand muscles. The SHTE algorithm was compared with other prominent methods such as the absolute hard threshold estimation (AHTE) algorithm, the statistical measures (SM) algorithm, and manual assessment. Results obtained in terms of robustness test and statistical analysis show that the proposed SHTE algorithm is reliable in estimating MEP latency, especially for the MEP signals having peak-to-peak (PTP) amplitudes lower than one hundred microvolts. Compared with the AHTE and SM algorithms, the SHTE shows a lower percentage deviation index in MEP latency estimation of the MEP signals with the PTP amplitudes lower than one hundred microvolts. Hence, the proposed SHTE algorithm represents an improved armamentarium in automatic MEP latency estimation.

INDEX TERMS Biomedical signal processing, digital signal processing, latency, motor evoked potential, transcranial magnetic stimulation.

I. INTRODUCTION

Since its introduction, which was more than thirty years ago [1], transcranial magnetic stimulation (TMS) has been extensively used as a non-invasive brain stimulation technique to explore cortical physiology in humans. In particular, single- and paired-pulse TMS protocols applied to the human primary motor cortex (M1) have allowed the physiological investigation of various intracortical inhibitory and facilitatory networks and cortico-cortical connectivity. As of recently, the TMS technique benefits from the integration of individual magnetic resonance images (MRIs) using navigation technology (navigated TMS or nTMS). The nTMS

The associate editor coordinating the review of this manuscript and approving it for publication was Gang Wang¹.

enables three-dimensional (3D) reconstruction of the brain surface based on the positioning of the stimulating coil over the M1 cortex and more precise electromyographic recording of motor evoked potential signals (MEPs) from the target muscles. Recording of MEPs allows measurement of corticospinal tract motor conduction time as a valuable diagnostic and investigation test in the routine practice of clinical neurophysiology [2], preoperative neurosurgery of the brain tumor surgery [3]–[7], epilepsy surgery [8]–[12], radiosurgical planning [13] or the surgical treatment of intracranial arteriovenous malformations [14]. Thus, MEPs elicited by TMS or nTMS over the human motor cortex provides a quantification of cortico-spinal excitability at the time of stimulation [15], [16]. The MEPs have been used and interpreted in several ways, each based on distinct assumptions

concerning cortico-spinal, intra- and trans-cortical contributions to MEPs, respectively [17]. Firstly, MEPs are interpreted concerning the performance of actions (resting-state vs. execution); secondly, to probe the physiology of the motor cortex (i.e., pharmacological manipulations or investigation of cortical excitability in the context of psychiatric or neurological illnesses) and thirdly, to probe the physiology that occurs outside of the M1.

The amplitude and the latency of the MEP signal are the most used features for quantifying MEP signals [17]–[19]. Although the MEP amplitude varies significantly in patients with pathologies, as well as in healthy subjects [18], [20]–[22], the peak-to-peak (PTP) amplitude defined as the difference between the maximum and minimum value of the MEP response, represents an accurate indicator for estimating the MEP amplitude oscillation [23]–[26]. On the other hand, the MEP latencies are considered more robust; however, MEP latency variability is well known in neurosurgical patients [18], [27]. Furthermore, in TMS protocols used for assessment of cortical inhibition (i.e., long/short-interval intracortical inhibition (LICI/SICI) or short-latency afferent inhibition (SAI)), suppression of MEP amplitude is detected [28]. This can challenge MEP amplitude detection and raise the problem of determining MEPs latency due to a higher signal-to-noise ratio. Most of the MEP latency estimation algorithms suffer from this problem, which significantly degrades detection precision, especially at the low PTP MEP signal amplitudes ($<100 \mu\text{V}$) [23]–[26].

Additionally, suppose a large number of signals have been collected in a clinic or research. In that case, it is essential to have an algorithm that will automatize a reliable estimate of such a large number of MEP signals, especially low amplitude. For that reason, the starting hypothesis of research presented in this work is that amplitude variability in the MEP signals can be used for comparing the robustness of individual algorithms dedicated to the estimation of MEP latency. Therefore, in this article, a newly developed algorithm named Squared Hard Threshold Estimator (SHTE) is proposed. It can be used for estimating the latency of MEP signals. The validation of the proposed algorithm was performed comparing the efficiency of the SHTE algorithm with other prominent algorithms and approaches based on MEPs manual assessment. To summarise, this article has a main contribution according to the following:

- We propose SHTE as a novel algorithm for MEP latency estimation.
- We perform a comparison of the proposed SHTE algorithm with other prominent MEP latency estimation algorithms. The robustness test and statistical analysis results show that the SHTE outperforms well-known algorithms in terms of latency estimation accuracy for the MEP signals with low amplitude.
- Based on the comparison results, it can be concluded that the proposed SHTE algorithm represents an additional method of choice in MEP latency analysis. SHTE can be

incorporated into clinical practice and research for faster and more precise latency estimation of MEP signals.

II. RELATED WORK ON CONTEMPORARY MEP LATENCY ESTIMATION ALGORITHMS

Previous medical studies show the variability of MEP latencies in the neurosurgical population undergoing preoperative nTMS mappings of the motor cortex [5], [18], [21]. The results of these studies pointed to a wide range of clinical factors (i.e., gender, height, age, drug intake, muscle-specific factors, tumor side, tumor location) that may impact MEP latency variability in nTMS motor mapping of brain tumor patients. However, some of the findings related to specific clinical factors on the MEP latency variability were not clarified [18]. Furthermore, the possible differences in the algorithms used to estimate the MEP latencies were also not questioned in past studies, and potential differences in latency computation impacted by the MEP signal amplitude value [5], [18].

Some of the previous studies related to the MEP latency estimation were based on measuring latency from the averaged rectified MEP records [29], [30]. Currently, the available algorithms for latency estimation can be divided into the following categories: algorithms based on *absolute hard threshold estimator* (AHTE), which are commonly used in devices of manufacturer Motometrics [23], and algorithms based on *statistical measures* (SM), which are widely used in devices of manufacturers Signal Hunter and CortexTools [24]–[26]. According to our knowledge, this work, for the first time, proposes a novel approach for estimating MEP latencies based on MEP signal squaring. To clarify differences among the proposed MEP latency estimation approach (SHTE), MEP estimation algorithms used by AHTE and SM approaches are described in further sections.

A. AHTE ALGORITHM

The execution of the AHTE algorithm relies on the following phases:

- a. Load the MEP and set a local coordinate system with the origin in the onset of the stimulus.
- b. Perform an absolute operation on the MEP using the following equation:

$$V_{abs(MEP)} = abs(x_1, x_2, \dots, x_n) \quad (1)$$

where $x \in \mathfrak{R}^m$ and $n \in \mathbb{N}^+$. x_n is recorded MEP signal obtained from the previous step.

- c. Find maximal absolute amplitude $V_{abs(max)}$, and determine the threshold value which is commonly set on 10% of $V_{abs(max)}$, i.e., $V_{thr} = 0.1 V_{abs(max)}$ where $V_{abs(max)}$ can be expressed with the following equation:

$$V_{abs(max)} = \sup(|x_1|, |x_2|, \dots, |x_n|) \quad (2)$$

- d. Mark $\pm 10\%$ level of $V_{abs(max)}$ area around the mean of the MEP signal and determine an index value (n_0) where the marked line crosses the MEP, i.e., at a first intersection where they have the same value.

- e. Use calculated index value (n_0) and subtract it from the so-called magic number (mn), to obtain a time instance as an estimation of the MEP latency (lat_{MEP}) according to Eq. 3:

$$lat_{MEP} = t(n_0 - mn) \quad (3)$$

A magic number (mn) is defined as a number that has a constant value, and it has to be subtracted from the index value (n_0) to determine the onset of MEP latency.

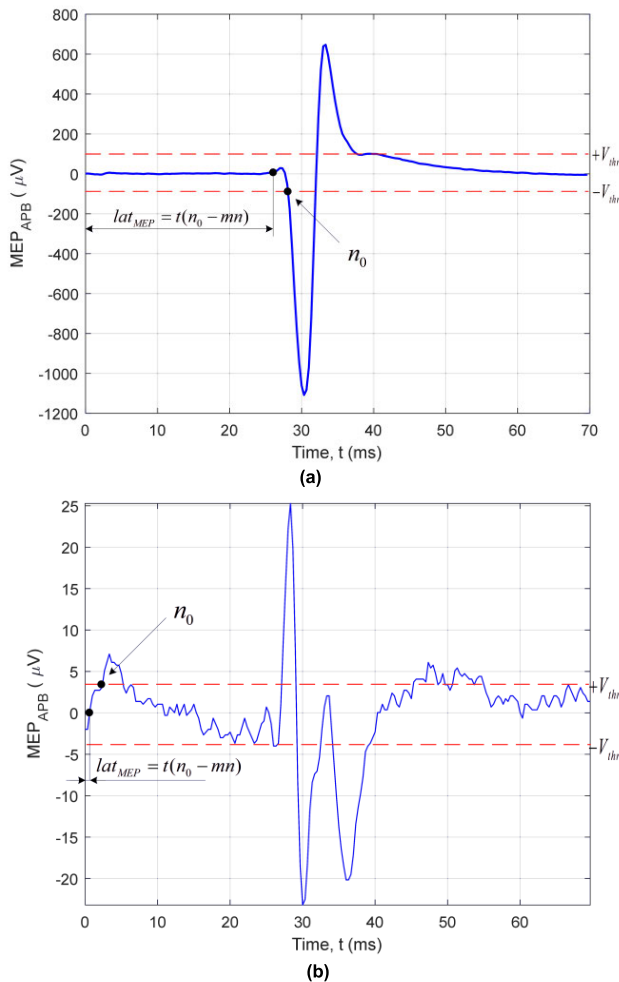


FIGURE 1. Estimation of MEP latency with the AHTE algorithm on two MEP signals: (a) MEP from the APB muscle with a latency of 25.5 ms and a PTP amplitude of 1.8 mV, (b) MEP from the APB muscle with a PTP amplitude of 50 μ V.

The presented AHTE algorithm is incorporated in the software of manufacturer Motometrics and has the option to change the threshold value V_{thr} [23]. In general, the AHTE method yields good results in determining MEP latency for the MEP signals with higher amplitudes. However, Fig. 1 illustrates the potential problem in estimating the MEP latency with the AHTE algorithm. Fig. 1 shows an example of two MEPs evoked from the hand muscle after applying a single magnetic stimulus to the M1. It is a typical MEP from the abductor pollicis-brevis (APB) muscle, with a latency

of 25.5 ms and a PTP amplitude of 1.8 mV. The index value (n_0) is determined at the intersection of the MEP and $-V_{threshold}$ dashed line, and the latency is estimated as a time instant where the index value is subtracted from the magic number [23].

Fig. 1b shows the MEP from the APB muscle with a PTP amplitude of 50 μ V. It can be observed that muscle response spans from 25 ms to 40 ms. Due to neurophysiologic processes in the human cortex and body, the activity from 0 ms to 25 ms and from 39 ms to 70 ms exhibits fluctuations that can be described as signal (muscle) noise. If the AHTE algorithm is applied, the index value (n_0) calculated at the intersection of the MEP and $+V_{thr}$ in Fig. 1b can be wrongly estimated in a presented practical example. More specifically, instead of 25 ms (Fig. 1a), the onset latency can be incorrectly estimated to 1 ms (Fig.1b). Hence, in some instances, characterized by noisy MEP signals, the MEP latency estimation becomes a very challenging task, and it can be significantly degraded in terms of accuracy.

B. ALGORITHMS BASED ON STATISTICAL MEASURES

Another approach used for the estimation of MEP latency is based on statistical measures (SM) algorithm. In general, the algorithms based on SM rely on the following steps:

- a. Load the MEP signal and set a local coordinate system with the origin in the stimulus onset.
- b. Perform moving average (MA) filtering for signal smoothing and noise reduction using the following equation:

$$MA(n) = \frac{1}{WL} \cdot (x_n + x_{n-1} + \dots + x_{n-(WL-1)}) \quad (4)$$

where $MA(n)$ denotes the moving-average filtering of a vector x . A moving-average filter slides a window of length (WL) along the data and computes averages of the data contained in the WL window size.

- c. Differentiate the smoothed signal to get a vector $Diff$ with the following equation:

$$Diff = [x_2 - x_1, x_3 - x_2, \dots, x_N - x_{N-1}] \quad (5)$$

where the elements of a $Diff$ are the differences between adjacent elements of the MEP. A vector $Diff$ is a vector of length $N - 1$, while the MEP signal has N elements.

- d. Calculate the standard deviation (SD) of the differentiated signal using the following equation:

$$SD = \sqrt{\frac{1}{N-1} \cdot \sum_{n=1}^N (x_n - \bar{x})^2} \quad (6)$$

where \bar{x} is a mean value of the differentiated signal.

- e. Set a threshold value to be equal to the value of SD multiplied with a constant k , i.e., $V_{thr} = k \cdot SD$.
- f. Compare each absolute differentiated value with the threshold value.
- g. Estimate the MEP latency onset as an index value (n_0), where the differential value first exceeds the threshold value and then subtract from a magic number (mn).

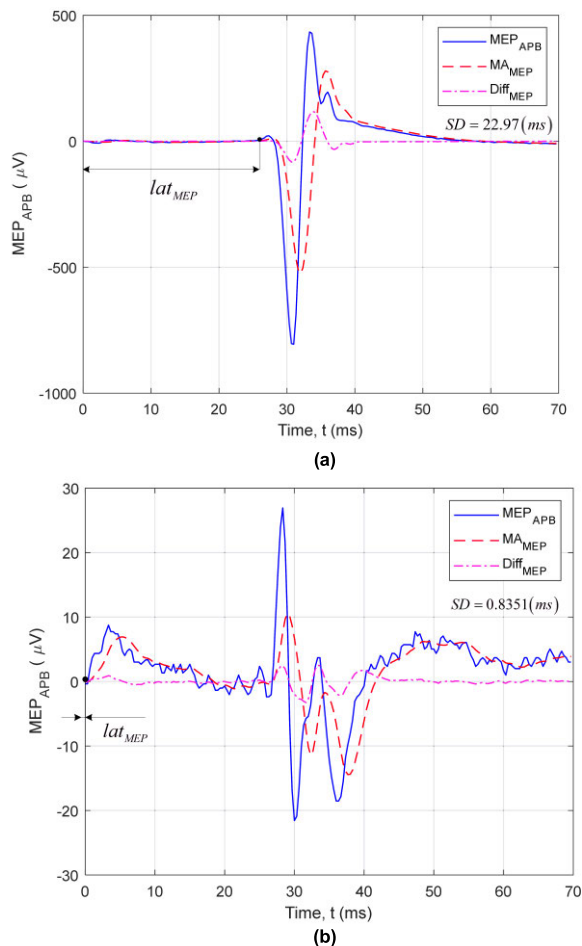


FIGURE 2. Estimation of MEP latency using the SM algorithm for (a) MEP signal with a PTP amplitude of 1.7 mV and latency of 27 ms, (b) MEP signal with a PTP amplitude of 49 μV and with an estimated latency of 1 ms.

For the case of the AHTE algorithm, the presented SM algorithm also yields good results in estimating the MEP latency for the MEP signals with higher PTP amplitudes but lacks accuracy for MEPs of lower PTP amplitudes. The reason can be found in the fact that on the lower PTP amplitudes, the noise is not negligible and has a significant impact on differentiation (step (c)). Then when applying the steps (d), (e), and (f) of the SM algorithm, it is possible that differentiated value can quickly exceed the thresholded value, as shown in Fig. 2. Although this cannot happen on higher PTP amplitudes due to the lower impact of noise, for lower amplitudes, this process is illustrated in Fig. 2. Fig. 2a shows a typical MEP signal (MEP_{APB}) that has a PTP amplitude of 1.7 mV and a latency of 27 ms.

Additionally, Fig. 2a shows the MA_{MEP} signal obtained through moving-average filtering (step (b)) and the signal $Diff_{MEP}$ derived from the differentiation process (step (c)). According to Fig. 2a, the standard deviation (SD) among signals after step (d) was 22.9 ms, and the threshold was set to 16.1 ms with $k = 0.7$. It can be observed that the MEP latency is correctly estimated in the case of higher PTP amplitudes.

However, Fig. 2b shows the MEP signal with a lower PTP amplitude of 49 μV and an estimated 1 ms latency. It can be observed that MA_{MEP} and $Diff_{MEP}$ in Fig. 2b significantly differ when compared with those for the high-amplitude MEP signal presented in Fig. 1a. Due to the described reasons, the SM algorithm makes a false latency estimation for this MEP signal. Also, a CortExTool [24], [25] is another application that uses a similar approach for the MEP latency estimation. It is based on taking all MEP signals and calculating an average of signals to get a so-called MEP EMG template [24]. A cross-correlation function between the prototype and the MEP signal in question is applied to estimate the MEP latency. However, the implemented cross-correlation function does not eliminate the latency estimate problem for low-amplitude signals.

Hence, all mentioned algorithms (AHTE and SM) give a relatively accurate estimation of the MEP signal latency with higher PTP amplitudes (exceeding 100 μV). However, a lower estimation (precision) rate is documented for the latency of the MEP signals with lower PTP amplitudes (i.e., lower than 100 μV) [18]–[22]. Therefore, there is a need for a better algorithm that will improve the latency estimation of MEP signals with lower PTP amplitudes. According to our knowledge, this article, for the first time, proposes a novel algorithm for improved detection of MEP signals having low PTP amplitudes.

III. SQUARED HARD THRESHOLD ESTIMATION

According to the evaluation overview of algorithms presented in the previous section (Section II), it is evident that nowadays protocols in neuroscience research and clinical medical fields (i.e., neurology, neurosurgery) are based on collecting and processing a large number of MEP signal records with varying amplitudes [18]. Sometimes, MEPs with lower amplitudes are not processed because the acquisition algorithms do not recognize them, or they are treated as muscle noise or outliers. For that reason, in this work, a novel SHTE algorithm is proposed to improve the MEPs latency estimation for PTP amplitudes lower than 100 μV . The block diagram presenting the five main steps (phases) of SHTE algorithm execution is shown in Fig. 3.

The first step of the SHTE algorithm execution is related to the loading of recorded MEP signal from the database and choosing the constraint parameters (Fig. 3). An example of the loaded MEP signal is presented in Fig. 4. According to Fig. 3, two constraint parameters are selected in the first step (Fig. 4): the length of the MEP signal for processing in the time domain (T_{WL}) and the so-called dropout zone (T_{DZ}) parameter. Fig. 4 shows that in the time domain, the length of the analyzed MEP spans from the onset of the stimulus (where the local coordinate system is set to 0 ms), to the end of the window length T_{WL} . In the presented analyses, the T_{WL} is set to 70 ms. The selection of T_{WL} value is justified through experimental analysis of many MEPs, as the time window within which all MEPs can be recorded. The dropout zone is a region that spans from the onset of the stimulus to the

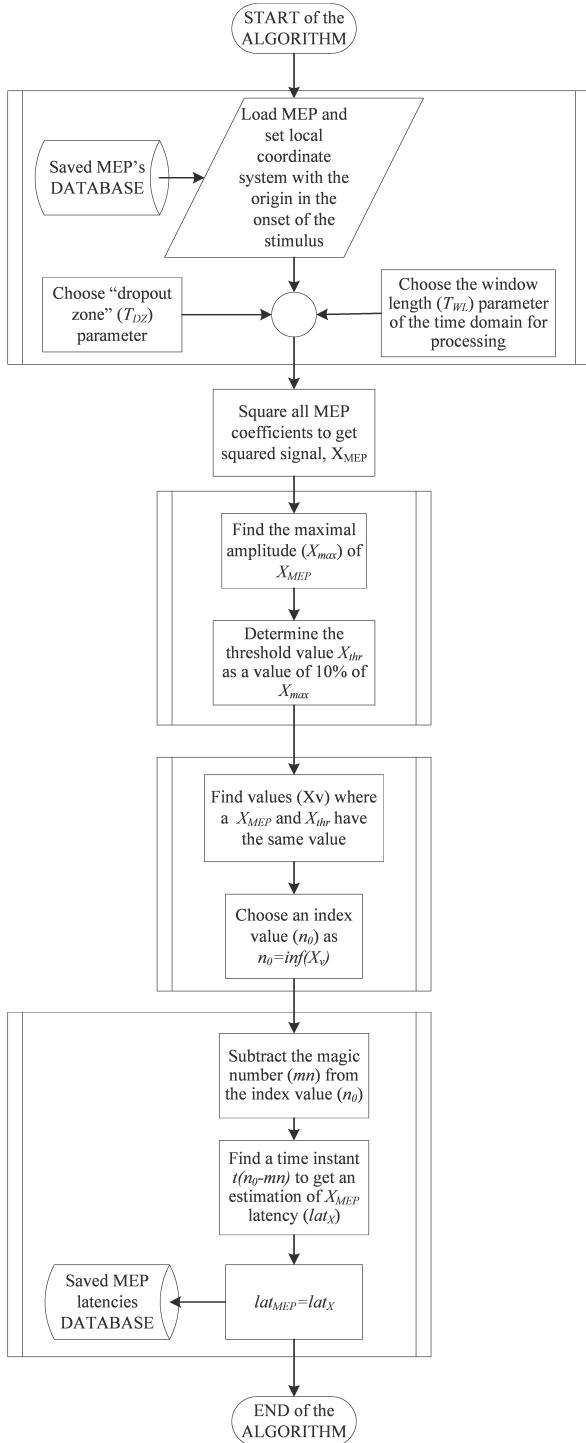


FIGURE 3. Proposed execution of the SHTE algorithm.

value of the predefined time T_{DZ} (Fig. 4). The value of T_{DZ} is selected as a measure that contributes to the increase of the latency estimation accuracy. The T_{DZ} is set to 19 ms due to the normative data defined for the MEP latency of the distal muscles [2]. Also, based on the results presented in [2], it is assumed that the mean MEP latency for the APB and first-dorsal interosseous (FDI) muscle is 20.8 ± 1.5 ms.

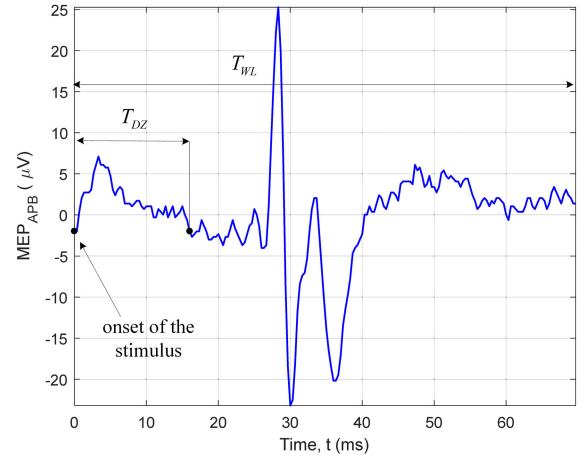


FIGURE 4. Loading the MEP signal and setting a local coordinate system.

In the second step of the algorithm execution, all amplitudes (coefficients) from the MEP signal are squared to get a squared coefficient (X_{MEP}) (Fig. 3).

Furthermore, in the third step of the algorithm execution, the following two operations are performed (Fig. 3): obtaining the maximal amplitude X_{max} of squared X_{MEP} signal and determining a threshold value X_{thr} through finding a 10% of X_{max} .

The fourth step of the algorithm execution performs the operation of finding an index value (n_0), which is defined as the signal level where X_{MEP} and X_{thr} are of the same value (Fig. 3). Since there are several instances where X_{MEP} and X_{thr} have the same value, and a minimum value is chosen as an index value.

To get an estimate of the MEP latency, in the last step of the SHTE algorithm execution (Fig. 3), the following procedures are performed: subtract the magic number (mn) from the index value and find a time instant $t(n_0-mn)$ for obtaining an estimate of X_{MEP} latency. Since squaring the coefficients of the MEP signal in the time domain have no impact on the MEP signal latency, it can be concluded that the estimated latency of the squared coefficient X_{MEP} is the same as the original MEP signal latency, i.e., $lat_{MEP} = lat_X$.

A. SHTE ALGORITHM

The performance characterization of the proposed SHTE algorithm with the mathematical backgrounds will be given on an arbitrary selected MEP signal presented in Fig. 1b. The proposed algorithm is executed in the following five steps (Fig. 3):

- a. Load MEP and set a local coordinate system with the origin in the onset of the stimulus (Fig. 4).
- b. Square all coefficients to obtain the squared coefficient

$$X_{MEP} = (x_1^2, x_2^2, \dots, x_n^2) \quad (7)$$

where $x \in \mathfrak{R}^m$, and $n \in \mathbb{N}^+$ what results with a squared signal (X_{MEP}), as presented in Fig. 5.

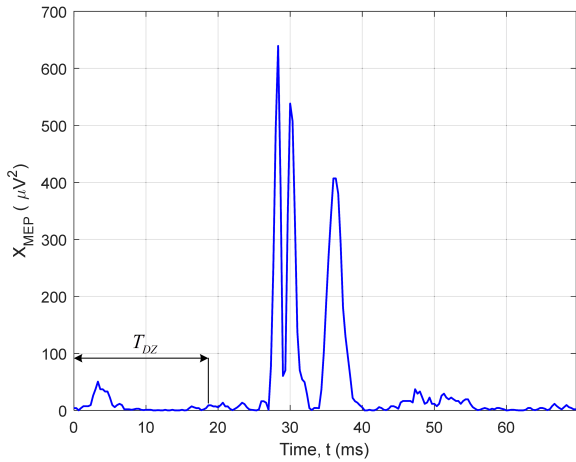


FIGURE 5. Squaring the MEP signal.

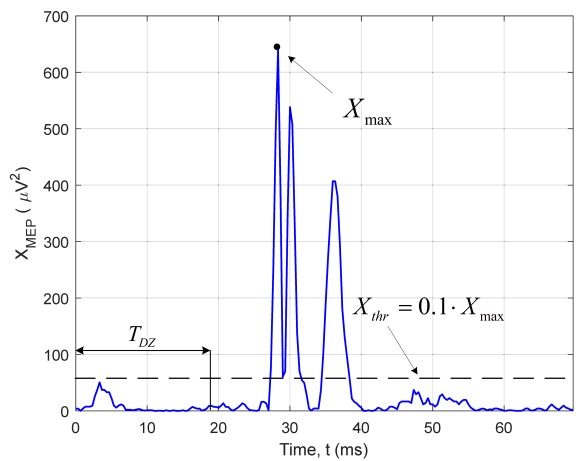


FIGURE 6. Finding the maximal amplitude and determining the threshold stripe.

- c. Find the maximal amplitude of squared coefficients using the following relation

$$X_{\max} = \sup(X_{MEP}) = \sup(x_1^2, x_2^2, \dots, x_n^2) \quad (8)$$

and then determine 10% of maximal amplitude (X_{\max}) threshold value (X_{thr}) such that

$$X_{thr} = 0.1 \cdot X_{\max} \quad (9)$$

The results of the performed signal processing procedure are shown in Fig. 6.

- d. Find an index value (n_0) where the threshold value (dotted line in Fig. 7) and the squared signal line are intersected and have the same value such that

$$X_{thr} = X_{MEP}(n_0) \quad (10)$$

The results of the process related to determining the index value are presented in Fig. 7. After performing the operation defined with (10), it can be seen that there are several intersection points. The index value iv is

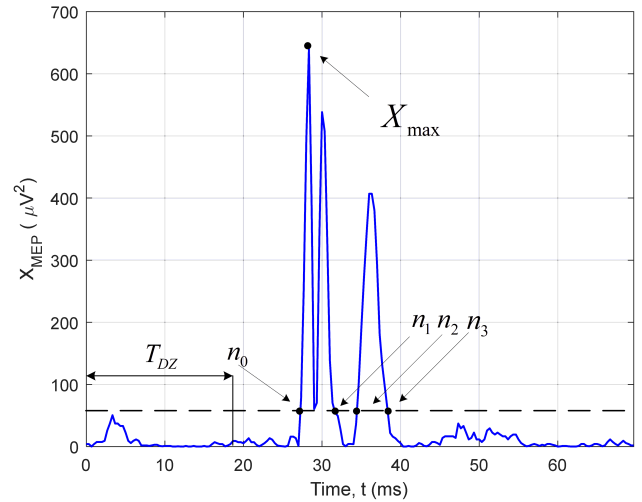


FIGURE 7. Determining the index value n_0 .

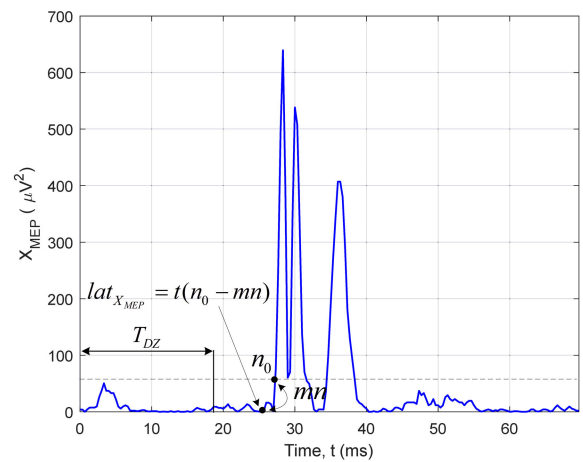


FIGURE 8. Finding the latency of the squared signal.

obtained by performing the next operation

$$iv = \inf(n_0, n_1, n_2, n_3) \quad (11)$$

were n_0, n_1, n_2, n_3 are the indices of intersections on the time axis. In this example, the selected index value is equal to n_0 .

- e. In order to find a time instant as an estimation of the latency of the squared signal, use the calculated index value (n_0) and subtract it from the magic number (mn) in order to be

$$lat_{X_{MEP}} = t(n_0 - mn) \quad (12)$$

The results of the performed process related to finding the squared signal's latency are shown in Fig. 8. According to the presented results, the latency of the MEP signal (Fig. 9) is the same as the estimated latency of the squared signal (Fig. 8).

Compared with other prominent algorithms, the novelty of the SHTE algorithm lies in squaring the amplitude of the

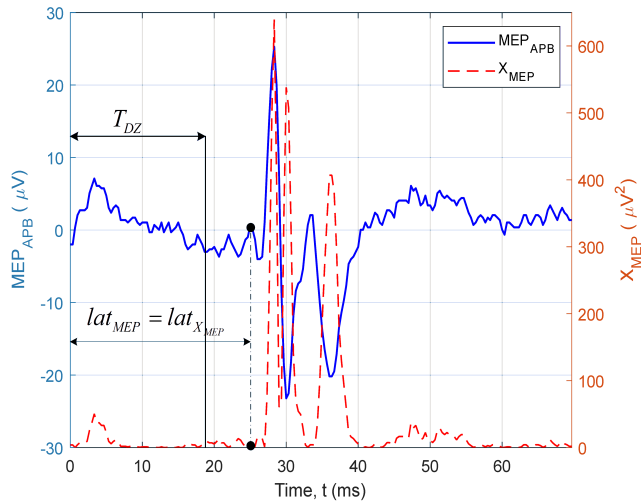


FIGURE 9. Overlapped the original MEP and squared the SHTE signal.

MEP signal (Fig. 5). Such squaring of the MEP signal ensures that the original signal coefficients' operations are transformed in the domain with squared coefficients. According to Fig. 8, higher PTP amplitudes that correlate with MEP muscle response time (from 25.5 ms to 40 ms) become distinctively greater (squared) than the squared amplitudes of the rest of the signal (the noise from 0 ms to 25.5 ms and from 40 ms to 70 ms). Also, applying the thresholding operation on a squared signal leads to a faster algorithm execution. This is a consequence of necessity related to finding only one threshold (a positive dashed line in Fig. 7), and no execution time is needed for the detection of the other part of the MEP signal related to the negative threshold value. At the same time, working with squared coefficients (Fig. 7 and Fig. 8) does not change the onset of the latency of an original MEP signal (Fig. 9).

IV. EXPERIMENTAL PROCEDURE FOR MEP SIGNAL ACQUISITION

Experimental evaluation of the proposed algorithm has been performed with the nTMS system (Nexstim NBS System 4 of the manufacturer Nexstim Plc.) on MEP signals collected from our recently published study investigating SAI phenomena of the motor cortex [31]. The SAI was investigated by a paired-pulse paradigm in which the electrical stimulation to the median nerve at the wrist is followed by single magnetic stimulation of the M1 with inter-stimulus intervals (ISIs) of 19 ms - 28 ms. The interval between the two magnetic pulses was 5 s. The control condition included magnetic stimulation over the M1 without conditioning electrical pulse.

The sample of 889 MEP signals was randomly pulled from the study [31], consisting of the control and ISIs condition. The MEP signals were acquired in 19 right-handed subjects (mean age 40.35 ± 14.4 SD) [31], [32]. In Fig. 10, an experimental procedure for obtaining MEP signals is illustrated. The MEPs were recorded from two hand muscles

(APB and FDI). The intensity of magnetic stimulation for the control condition was 120% of the resting motor threshold (RMT) intensity, and at ISIs between 19 ms and 28 ms, magnetic stimulation intensity was also 120% of the RMT. The control condition at ISIs included ten trials for each subject. The lowest stimulation intensity used to elicit at least five positive MEP responses out of ten trials having PTP amplitudes larger than $50 \mu V$, was defined as the RMT intensity [2].

The MEPs were recorded with a pair of self-adhesive surface electrodes (Ambu [®]Blue Sensor BR, BR-50-K/12 of manufacturer Ambu A/S) in a belly-tendon montage (Fig. 10). Electrodes were attached to the electrode cable of the Nexstim EMG with a 1.5 mm touch-proof female safety connector (DIN 42-802) and connected to a 6-channel EMG and one common ground EMG amplifier (external module) with TMS-artefact rejection circuitry. The EMG is an integrated part of the nTMS device.

TABLE 1. Values of experimental parameters used for MEP signal acquisition.

Experimental parameter	Value
EMG	
Sampling frequency (F_s) per channel	3kHz
Resolution	$0.3 \mu V$
Scale	between -7.5 mV and 7.5 mV
Common-mode rejection ratio (CMRR)	> 90 dB
Peak-to-peak noise	$< 5 \mu V$
Frequency band	range of 10-500 Hz
TMS stimulation parameters	
Pulse	single
Pulse width	$289 \mu s$
Stimulation intensity	120 % from the RMT
Electrical stimulation parameters	
Pulse	single
Pulse duration	$200 \mu s$
Intensity of stimulation	6 mA

Table 1 presents the characteristics of the EMG with parameters of the magnetic and electrical stimulation. Electrical stimuli consisted of single pulses (of $200 \mu s$ duration) (Table 1) applied through a stimulating electrode to the median nerve applied at the wrist of the right hand (Fig. 10). The stimulating bar electrode (manufactured by ADInstruments) had flat disks and the 30 mm spacing of 9 mm contacts of the anode which was positioned distally. For median nerve stimulation, the ISIs Neurostimulator (version 1.0.2.0. of manufacturer Inomed Medizintechnik GmbH) was used to ensure constant current stimulation.

Before nTMS experiment, the MRI of the head for each subject was performed with Siemens Magnetom Area (of the manufacturer Siemens Healthcare GmbH) having Tim (76×18) of strength 1.5 T. MRI images were used for the 3D reconstruction of individual brain anatomy (3D optical tracking unit of the manufacturer Polaris [®]Vicra) [33]. With the subject comfortably seated, the MRI is co-registered to the subject head using the tracking system with Nexstim

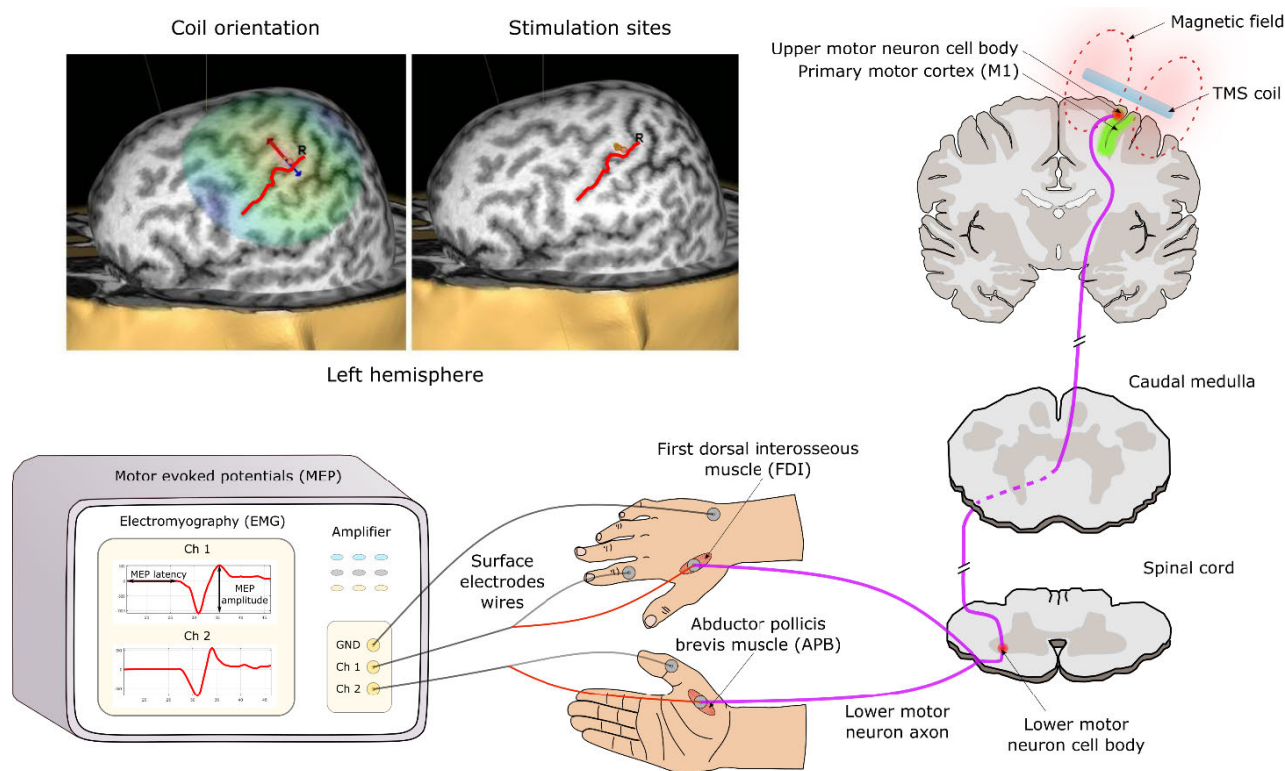


FIGURE 10. The procedure of the TMS experiment for collecting MEP signals.

unique forehead tracker. When resting the coil against the subject head, the electric field is overlaid on the 3D model of the brain. As the coil is moved, the magnitude (V/m) and orientation of the electric field relative to the cortex are dynamically calculated and displayed in real-time. The eight-shaped magnetic coil was used, generating a biphasic pulse having a length of $289 \mu s$ (Fig.10, Table 1). The coil with an inner winding diameter of 50 mm and an outer winding diameter of 70 mm was placed tangentially to the subject skull over the M1 (Fig. 10). The maximum strength of the electric field measured 25 mm below the coil in a spherical conductor model representing the human head was 172 V/m [34].

The direction of the coil orientation over the precentral gyrus and stimulation sites is presented in the top left part of Fig. 10, for the left M1 of the single-subject APB muscle. The central sulcus is depicted in the red color line on the upper left part of Fig. 10. The top right and bottom right in Fig. 10 shows the TMS coil located tangentially to the skull over the left M1. A time changing current in the coil generates a time changing magnetic field, which induces an electric field that depolarizes the upper motor neurons with corticospinal efferents. This action potentials from the upper motor neurons excite the lower motor neurons in the spinal cord (Fig. 10), whose action potentials travel through the peripheral nerves to the target muscles in the form of MEP signals.

The SAI approach enables suppression of amplitude of MEP signals when the median stimulation precedes

a magnetic stimulation applied to the motor cortex, which results in SAI [28], [35]. In the present study, to obtain a robust sample of signals for the SHTE algorithm validation, the SAI protocol was chosen for the collection of MEP signals with variable PTP amplitudes.

The factors such as the cleanliness of the skin, usage of the disposable electrodes, etc. that might interfere with MEP characteristics (such as noise) during nTMS mapping were minimized [1], [28].

V. SHTE ALGORITHM VALIDATION

The following procedure was conducted to validate the SHTE algorithm. The three algorithms (SHTE, AHTE, and SM) were compared in terms of performance. Also, SHTE, AHTE, and SM algorithms were validated with the manual assessment, being the reference method in estimating MEP latency. Hence, in total, the amplitude and latency of 889 MEP signals were estimated with SHTE, AHTE, and SM algorithms and manually with the custom-made script written in Matlab 2019a. The MEP signals acquired from APB and FDI muscles were analyzed jointly since the same median nerve innervates both muscles. It is reasonable to assume that a sample of 889 MEPs (551 from APB and 338 from FDI) of different PTP amplitude ensures a robust and relevant sample for performing reliable analyses.

A. STATISTICAL DATA ANALYSES

Statistical data analysis was performed in the following manner to validate the SHTE algorithm. The 889 MEP signals

were grouped into two amplitude bands. More specifically, MEP signals with a PTP amplitudes from 0 μV to 100 μV (denoted as $V_{pp} < 100 \mu\text{V}$) and MEP signals with a PTP amplitude above 100 μV (marked as $V_{pp} > 100 \mu\text{V}$). Among 889 MEP signals, 388 MEP signals were grouped in $V_{pp} < 100 \mu\text{V}$ amplitude band and the remaining 501 MEP responses were grouped in $V_{pp} > 100 \mu\text{V}$ amplitude band. Additionally, 388 MEP signals with $V_{pp} < 100 \mu\text{V}$ have been divided into two amplitude bands: 132 MEP signals with PTP amplitude from 0 μV to 50 μV (denoted as $V_{pp} < 50 \mu\text{V}$) and 256 MEPs with PTP amplitude from 50 μV to 100 μV (marked as $50 \mu\text{V} > V_{pp} < 100 \mu\text{V}$).

The *post hoc* G power test was performed to determine does such amplitude band grouping was adequate for two-way analyses of variance (ANOVA). G power for amplitude bands $V_{pp} < 100 \mu\text{V}$ and $V_{pp} > 100 \mu\text{V}$, as well as for $V_{pp} < 50 \mu\text{V}$ and $50 \mu\text{V} > V_{pp} < 100 \mu\text{V}$ was 0.9. The post hoc G power test results show that the estimated power confirmed the adequacy of MEP signal grouping in each PTP amplitude band.

Then, the statistical data analysis was conducted using the STATISTICA 12 tool (of manufacturer StatSoft Inc.). For statistical data analyses, a Student t-test with independent samples was used to determine if two examiners differ in their manual estimation of MEP latency. The ANOVA was conducted to test the differences in MEP latency values for $V_{pp} < 100 \mu\text{V}$, $V_{pp} > 100 \mu\text{V}$, $V_{pp} < 50 \mu\text{V}$, and $50 \mu\text{V} > V_{pp} < 100 \mu\text{V}$ amplitude bands for four different approaches (SHTE, AHTE, SM, and manual estimation). The percentage deviation index (PDI) measure was used to evaluate and compare the efficiency of SHTE, AHTE, and SM algorithms in MEP latency estimation. For calculating PDI, the average expert’s assessment (manual assessment expressed as lat_{man}) of MEP latency was used as a reference for expressing PDI as

$$PDI[\%] = \frac{|lat_{SHTE/AHTE/SM} - lat_{man}|}{lat_{man}} \cdot 100 \quad (13)$$

were $lat_{SHTE/AHTE/SM}$ denotes estimated MEP latency by SHTE, AHTE or SM algorithm, respectively.

To determine if SHTE, AHTE and SM distinguish from the manual assessment of two examiners in the process of MEP latency estimation, two-way ANOVA was used on PDI results with two amplitude bands, more specifically PTP amplitude bands $V_{pp} < 100 \mu\text{V}$ and $V_{pp} > 100 \mu\text{V}$, and PTP amplitude bands $V_{pp} < 50 \mu\text{V}$ and $50 \mu\text{V} > V_{pp} < 100 \mu\text{V}$, respectively. In the frame of the two-way ANOVA method, F-tests were used to statistically test the effect of the independent variables (used methods and MEP amplitudes) on the expected outcome (PDI values). Also, analyses take into account the effect of independent variables and their relationship to the outcome itself. F-test statistic presents a ratio of two variances, which is a measure of dispersion, or how far the data are scattered from the mean value. In the case of significant depressions, the Fisher Least Significant Difference (FLSD) *post hoc* test was calculated. The distinction was

considered statistically significant when difference probability p is equal to $p < 0.001$. In the Results and Discussion sections, these descriptive statistics were displayed in the form of arithmetic mean, SD, and minimal and maximal divergence percentages.

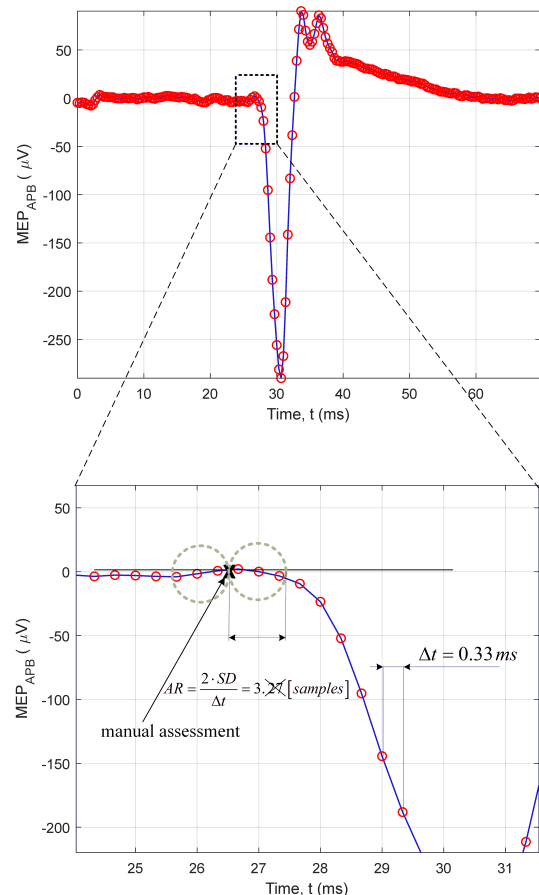


FIGURE 11. An example of a typical MEP signal with the magnification of the latency onset area.

B. MANUAL ASSESSMENT APPROACH

Two facts have been taken into account when comparing SHTE, AHTE, and SM with the manual assessment. First, a manual evaluation based on an expert assessment is a continuous process for the MEP signal latency estimation. For example, Fig. 11 shows the MEP signal and the magnification of the latency onset area. An expert assessment of the MEP signal latency can be between the two samples (marked as “X” in the magnified part of Fig. 11), and hence, an expert can estimate the MEP latency at any point on the MEP signal. On the contrary, the estimation performed by each algorithm is based on MEP samples, which were recorded as discrete samples (red circles in Fig. 11) with a sampling frequency F_s of 3 kHz. Therefore, some uncertainty when dealing with the MEP latency estimation also exists in the time domain. Such uncertainty, which is called accuracy region (AR) is equal to a certain number of samples around the “true”

value assessed manually (presented with the two green dotted circles in Fig. 11).

For example, for $F_s = 3$ kHz, the time resolution (Δt) between the two samples is equal to 0.33 ms ($\Delta t = 0.33$ ms). This means that AR between manual latency estimation and an algorithm estimation can have at least 0.33 ms error, which is equivalent to AR of one sample (AR1). Taking into account that the SD between the experts performing manual assessment was 0.54 ms, for estimating uncertainty in performance assessment, the value of two SDs was taken as a measure of AR. This means all estimated latencies (by algorithms) in the AR are around 1.1 ms, which equals to 3.27 samples ($(2 \cdot SD)/\Delta t$). This explains why AR was set to three samples (next larger integer number), and this value of samples (AR3) is used as an AR value that assumes estimated latencies accurate (Fig. 11).

C. SELECTION OF MAGIC NUMBER

The selection of a magic number (mn) also represents an important factor in achieving satisfactory estimation accuracy. The magic number (mn) is a constant number that must be subtracted from the index value (n_0) when determining the onset of MEP latency. The following methodology was used to determine the magic number. From the origin of the MEP signal, time instances corresponding to the point of 10% and 20% of V_{max} were determined. Then, the least squared method was applied to substitute the portion of the signal with a linear, quadratic or exponential polynomial. Following the calculation of r-squared and adjusted r-squared measures, the best fit polynomial was determined. After determining the polynomial that best fits the MEP signal's portion, the exact number of samples between them was counted and subtracted, determining the onset of the MEP signals.

Performed analyses show that the magic number lies between four and six samples, and for testing the AHTE algorithm, it was set to five samples. Since the SHTE algorithm transforms MEP signal coefficients into squared signal coefficients, there is a difference of 31.6% between a "regular" and "squared" domain. This difference corresponds to the value of magic number equal to 6.6, and due to the necessity of selecting the next highest integer value, it is set to seven for the analyses. Hence, the proposed SHTE algorithm subtracts seven samples from the index value to determine the MEP signal's onset and then finds the time instance to estimate the latency.

D. ROBUSTNESS TEST

Besides statistical data analysis, the robustness test was performed, and a number of hits (NOH) were used as a measure for validating the SHTE algorithm. The NOH represents the number of correctly MEP latency estimations among the total number of MEP signals in the specific amplitude band. The equation used for the NOH measure is:

$$NOH[\%] = \frac{\text{number of hits}}{\text{total number of signals in ampl.band}} \quad (14)$$

The NOH analysis is performed as a complement to a robustness test since the NOH analysis arises directly from the robustness analysis. The robustness test for SHTE, AHTE, and SM algorithms is performed in two phases. First, 889 MEPs are divided into two amplitude bands, the amplitude band with $V_{pp} < 100 \mu V$ and the amplitude band with $V_{pp} > 100 \mu V$. Second, out of the total number of MEPs in each amplitude band, ten groups are created. More specifically, each group forms 10% of the total number of MEP signals of that group up to 100% of the total number of MEP signals. Each group consists of the 30 sets of randomly collected MEPs from the observed amplitude band. For each measurement, the MEP latency from AR1 to AR5 is estimated for all three algorithms (SHTE, AHTE, and SM). Then, from AR1 to AR5 for each group, an average NOH is calculated. All data are presented as percentage values.

Finally, for each algorithm, measures such as minimum NOH value of all groups (Min.), maximum NOH value of all groups (Max.), total NOH average of all groups (Average) and standard deviation of NOHs for all groups (SD) are determined. In addition, the time execution of SHTE, AHTE, and SM algorithms were assessed. First, 410 MEP signals were randomly collected. Then, the execution of each algorithm was performed sequentially in 15 series. Finally, the average execution time of each algorithm was calculated.

TABLE 2. Mean values (\pm SD) of MEP signal latency for AHTE, SHTE, SM algorithms, and manual assessment in different amplitude bands.

MEP Amplitude (μV)	Methods				No. of signals
	AHTE MEP latency (ms)/S D (ms)	SHTE MEP latency (ms)/S D (ms)	SM MEP latency (ms)/S D (ms)	Manual MEP latency (ms)/S D (ms)	
< 50	19.3 (1.9)	20.5 (3.1)	4.6 (9.2)	23.2 (1.7)	132
50-100	21.0 (2.8)	23.4 (2.9)	13.6 (11.7)	23.7 (1.8)	256
0-100	20.3 (2.7)	22.4 (3.3)	10.5 (11.7)	23.5 (1.8)	388
> 100	23.3 (2.2)	23.7 (2.1)	23.7 (3.5)	23.5 (2.0)	501

VI. RESULTS

Obtained results indicate no significant differences between manual examiners when estimating MEP latency ($t = 1.13$, $p > 0.05$). Therefore, the examiners assessment values were averaged, and mean values are used in the further analysis as benchmark parameters of manual assessment results. Statistics of MEP latency in two amplitude bands ($V_{pp} < 100 \mu V$ and $V_{pp} > 100 \mu V$) for SHTE, AHTE, SM algorithms, and manual assessment methods are presented in Table 2.

In Fig. 12, the PTP amplitude distribution of 889 MEP signals divided into two amplitude bands, $V_{pp} < 100 \mu V$ (Fig. 12a) and $V_{pp} > 100 \mu V$ (Fig. 12b) are presented. Fig. 12 shows the normal distribution and skewness trends of PTP MEP signal amplitudes for these two amplitude bands.

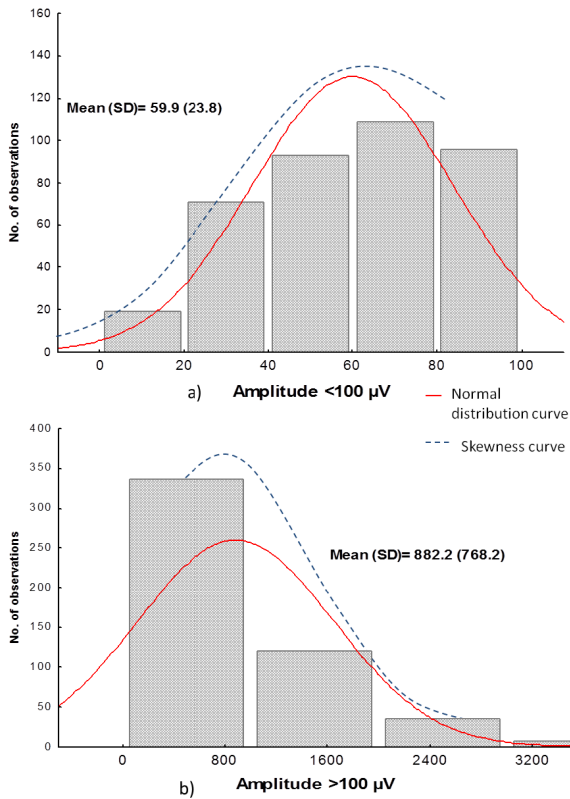


FIGURE 12. MEP PTP amplitude distribution of 889 signals for: a) amplitude band $V_{pp} < 100 \mu V$ ($N_{<100\mu V} = 388$), b) amplitude band $V_{pp} > 100 \mu V$ ($N_{>100\mu V} = 501$).

Significant differences were found between MEP signals with $V_{pp} < 100 \mu V$ and $V_{pp} > 100 \mu V$ ($t = -21.08$, $p < 0.001^*$). Additionally, ANOVA results for MEP signal latencies indicate notable differences concerning amplitude bands and signal processing methods ($F_{amplitude} = 304.3$, $p < 0.001^*$; $F_{method} = 384.6$, $p < 0.001^*$; $F_{interaction} = 398.1$, $p < 0.001^*$). The Fisher LSD *post hoc* test further revealed differences between SHTE and AHTE ($p < 0.001^*$) and SHTE and SM algorithms ($p < 0.001^*$) for MEP amplitudes with $V_{pp} < 100 \mu V$. Also, differences in SM and manual assessment ($p < 0.001^*$), as well as in AHTE and manual assessment for MEP amplitudes with $V_{pp} < 100 \mu V$ have been observed. Hence, results indicate significantly lower MEP latency of of SM algorithm when compared with manual estimation, SHTE algorithm, and AHTE algorithm, for MEPs with $V_{pp} < 100 \mu V$.

Furthermore, Table 3 and Fig. 13 present the PDI results for the AHTE, SHTE, and SM algorithms and manual assessment for $V_{pp} < 100 \mu V$ and $V_{pp} > 100 \mu V$ PTP amplitude bands. The two-way ANOVA was conducted for PDI of MEP latency using manual assessment as a reference point. Obtained results of F-tests and Fisher's LSD *post hoc* tests ($F_{methods} = 450.7$, $p < 0.001^*$; $F_{amplitude} = 531.3$, $p < 0.001^*$; $F_{interaction} = 394.2$, $p < 0.001^*$; *post hoc* SM-AHTE $< 100 \mu V$, $p < 0.001^*$; SM-SHTE $< 100\mu V$, $p < 0.001^*$; AHTE-SHTE $< 100 \mu V$, $p < 0.001^*$) confirm the statistical

TABLE 3. Mean percentage deviation index (PDI) and standard deviation (SD) of mep signal latency estimation for shte, ahte, and sm algorithms.

MEP Amplitude (μV)	Methods		
	AHTE (%)	SHTE (%)	SM (%)
<50	17.7 (8.8)	13.1 (11.3)	80.9 (37.5)
50-100	11.8 (11.3)	5.3 (7.4)	45.3 (46.8)
0-100	13.85(10.9)	7.9 (9.7)	57.4 (47.0)
>100	2.12 (4.3)	1.8 (2.7)	3.7 (11.5)

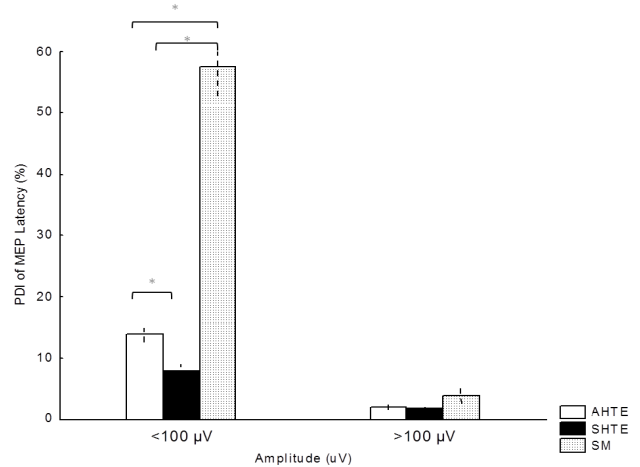


FIGURE 13. The percentage deviation of MEP latency estimation for SHTE, AHTE, and SM algorithms compared to manual assessment for the 889 MEP signals divided into two PTP amplitude bands ($V_{pp} < 100 \mu V$ and $V_{pp} > 100 \mu V$).

difference of PDI mean values. Compared to other algorithms, the SHTE has the lowest mean values in amplitude range from $0 \mu V - 100 \mu V$ (denoted as $V_{pp} < 100 \mu V$) (Table 3). This confirms the SHTE algorithm stability in detecting MEP latency for the MEP signals with PTP amplitude lower than $100 \mu V$ ($V_{pp} < 100 \mu V$).

Table 4 presents the results of NOH and robustness test for MEP latency estimation of SHTE, AHTE, and SM algorithms in $V_{pp} < 100 \mu V$ and $V_{pp} > 100 \mu V$ amplitude bands. Table 7 to Table 18 in the Appendix present the results of robustness testing of SHTE, AHTE, and SM algorithms for MEP latency estimation in each amplitude band: $V_{pp} < 50 \mu V$ (Tables 7-9 in the Appendix), $50 \mu V > V_{pp} < 100 \mu V$ (Tables 10-12 in the Appendix), $V_{pp} < 100 \mu V$ (Tables 13-15 in the Appendix), and $V_{pp} > 100 \mu V$ (Tables 16-18 in the Appendix). The robustness test in the amplitude band $V_{pp} < 100 \mu V$ is performed for 388 of MEPs (Tables 13-15 in the Appendix). Therefore, the sample size was varied from 39 MEP signals (the 10% of all 388 MEP signals) to 388 MEPs (the 100% of 388 MEP signals). From Table 4, it can be seen that the SHTE and AHTE algorithms perform robustly in all ARs, while the SM algorithm performs robustly in AR1, AR3, and AR4, and less robustly in AR2 and AR5. For example, in AR2, the SM algorithm,

TABLE 4. Results of the robustness tests for MEP signal latency estimation on SHTE, AHTE, and SM algorithms in PTP amplitude bands $V_{pp} < 100 \mu V$ and $V_{pp} > 100 \mu V$.

AR (Samples) (Time res.)	$V_{pp} < 100 \mu V$ (388 MEPS)					$V_{pp} > 100 \mu V$ (501 MEPS)				
	1 (0.4ms)	2 (0.7ms)	3 (1.1ms)	4 (1.5ms)	5 (1.9ms)	1 (0.4ms)	2 (0.7ms)	3 (1.1ms)	4 (1.5ms)	5 (1.9ms)
	SHTE					SHTE				
Avg. NOH (%)	36.5	54.4	63.4	67.5	71.0	64.2	79.5	88.4	95.5	97.5
SD	0.5	0.2	0.5	0.6	0.6	0.3	0.2	0.3	0.3	0.3
Min.	35.9	54.2	62.9	67.1	70.2	63.6	79.0	88.0	94.8	96.8
Max.	37.8	54.8	64.7	68.9	72.6	64.6	79.9	89.1	95.7	97.9
	AHTE					AHTE				
Avg. NOH (%)	23.4	31.8	36.5	38.1	42.2	70.0	83.7	89.8	94.4	95.9
SD	0.6	0.4	0.4	0.4	0.4	0.5	0.3	0.4	0.3	0.3
Min.	22.1	31.0	35.8	37.3	41.3	69.0	82.9	89.0	93.8	95.4
Max.	24.5	32.5	37.0	38.8	42.7	70.6	84.1	90.3	94.8	96.2
	SM					SM				
Avg. NOH (%)	18.4	29.7	34.4	38.1	40.6	54.3	78.7	85.6	92.6	96.8
SD	0.4	0.7	1.0	0.8	0.9	0.5	0.3	0.2	0.3	0.2
Min.	17.9	28.2	32.1	36.2	38.6	53.7	78.2	85.3	92.0	96.3
Max.	19.1	30.6	35.4	39.0	41.9	55.5	79.2	86.1	92.9	97.0

on average, has a score of 29.7 (± 0.7 , SD)% NOHs with the minimum and maximum NOH values of 28.2% and 30.6%, respectively. This means that the SM algorithm can usually correctly estimate two out of ten MEP latencies. It could accurately estimate an additional MEP latency in some very rare cases, i.e., it could accurately estimate three out of ten MEP signal latencies. If another solution space, i.e., when the AR3 is examined, it can be seen that the SHTE algorithm outperforms AHTE and SM algorithms in terms of accurate MEP signal latency estimation. On average, the SHTE has six out of ten, while both the AHTE and SM algorithms have three out of ten correct MEP signal latency estimates. It can be seen that analyzed algorithms perform robustly in AR3, regardless of varying the number of sample size. Also, compared with AHTE and SM, the SHTE algorithm scores even better if the AR is expanded. For instance, in the AR5, the SHTE has seven out of ten correctly estimated MEP latencies, while the AHTE and SM have four out of ten accurately estimated latencies.

To summarize, the SHTE outperforms AHTE and SM algorithms in terms of accuracy of MEP latency estimations in the PTP amplitude band $V_{pp} < 100 \mu V$. Furthermore, in the amplitude band $V_{pp} > 100 \mu V$, the robustness test is performed on the sample size of 501 MEP signals (Tables 16-18 in the Appendix). From Table 4, it can be seen that the SHTE and SM perform robustly over all ARs, while the AHTE performs robustly over AR2, AR4, and AR5, and less robustly on AR1 and AR3. If AR3 is examined, all three algorithms correctly estimate eight out of ten MEP signal latencies. However, sometimes the AHTE could accurately estimate an additional MEP latency (see Table 17 in the Appendix), due to the max. value on NOHs that is 90.3%. On average, the SHTE scores 88.4 (± 0.3 , SD)% NOHs,

TABLE 5. NOH results on SHTE, AHTE and SM algorithms for MEP signal latency estimation of all MEP PTP amplitudes.

AR (Samples) (Time res.)	All MEP PTP amplitudes				
	1 (0.4ms)	2 (0.7ms)	3 (1.1ms)	4 (1.5ms)	5 (1.9ms)
	SHTE				
NOH	305	407	462	498	515
Total	612	612	612	612	612
NOH (%)	49.9	66.5	75.4	81.3	84.1
	AHTE				
NOH	281	350	384	403	420
Total	612	612	612	612	612
NOH (%)	45.9	57.2	62.7	65.8	68.6
	SM				
NOH	220	328	364	398	419
Total	612	612	612	612	612
NOH (%)	35.9	53.7	59.5	65.0	68.4

the AHTE scores 89.8 (± 0.4 , SD)% NOHs and the SM scores 85.6 (± 0.3 , SD)% NOHs. If the AR1 is observed, the AHTE despite the average NOHs of 70.0 (± 0.5 , SD)% could correctly estimate one less MEP latency (min. NOH value is 69.0%), when the sample size is 151 or 301 MEP signals (Table 17 in the Appendix). Hence, all analyzed algorithms work well for the amplitude band $V_{pp} > 100 \mu V$ in AR3 as the solution space. NOH performance of SHTE, AHTE, and SM algorithms in MEP latency estimation for all MEP PTP is shown in Table 5.

To estimate the NOH performance of SHTE, AHTE, and SM algorithms for all MEP PTP amplitudes (Table 5), the following analysis was performed. For the amplitude bands $V_{pp} < 100 \mu V$ and $V_{pp} > 100 \mu V$, approximately the same number of MEP signals are chosen. The robustness test has

TABLE 6. Results of the robustness test for MEP latency estimation on SHTE, AHTE, and SM algorithms in amplitude bands $V_{pp} < 50 \mu V$ and $50 \mu V > V_{pp} < 100 \mu V$.

AR (Samples) (Time res.)	$V_{pp} < 50 \mu V$ (132 MEP signals)					$50 \mu V > V_{pp} < 100 \mu V$ (256 MEP signals)				
	1 (0.4ms)	2 (0.7ms)	3 (1.1ms)	4 (1.5ms)	5 (1.9ms)	1 (0.4ms)	2 (0.7ms)	3 (1.1ms)	4 (1.5ms)	5 (1.9ms)
	SHTE					SHTE				
Avg. NOH (%)	23.7	37.3	41.0	44.8	47.0	42.8	63.4	74.6	78.8	82.9
SD	0.6	0.8	0.9	0.7	0.7	0.6	1.3	1.0	0.5	0.4
Min.	22.9	35.6	38.8	43.1	45.2	41.7	62.0	73.8	77.9	82.7
Max.	24.5	37.9	42.2	45.7	47.7	44.0	66.8	77.1	79.7	84.0
	AHTE					AHTE				
Avg. NOH (%)	9.1	13.0	14.5	14.5	20.6	31.4	41.9	48.4	50.6	53.7
SD	0.6	0.6	0.6	0.6	0.5	1.0	1.1	1.0	0.7	0.4
Min.	8.5	12.0	13.8	13.8	19.8	30.3	40.7	47.1	49.6	53.0
Max.	10.5	14.3	16.0	16.0	21.2	33.8	44.6	50.6	52.1	54.5
	SM					SM				
Avg. NOH (%)	6.8	14.2	14.2	16.5	17.3	24.7	37.7	44.9	49.3	52.8
SD	0.4	0.5	0.5	0.5	0.5	0.4	0.7	0.5	0.8	0.5
Min.	6.0	13.3	13.3	15.8	16.5	23.8	36.8	44.1	48.5	52.2
Max.	7.4	15.0	15.0	17.3	18.1	25.5	39.5	45.8	51.2	53.8

been performed with 311 MEP signals for the amplitude band $V_{pp} < 100 \mu V$, and the average NOHs are calculated. Also, the same test was performed with 301 MEP signals in the amplitude band $V_{pp} > 100 \mu V$. Then, the results obtained from both amplitude bands are used to create the NOH table in MEP signal latency estimation for all MEP PTP amplitudes. From Table 5 can be seen that there was a total of 612 MEP signals. Due to the fact that the robustness test was performed, a total of 889 MEP signals were used to determine the performance of all three algorithms. It can be observed that the SHTE algorithm has the best MEP latency estimation in all ARs. For example, if AR3 is examined, on average, the SHTE accurately estimates seven out of ten MEP signal latencies (75.4% NOHs), while the AHTE correctly estimates six out of ten MEP latencies (62.7% NOHs). Furthermore, the SM accurately estimates five out of ten MEP latencies (59.5% NOHs).

Statistics of MEP latency analyses in amplitude bands $V_{pp} < 50 \mu V$ and $50 \mu V > V_{pp} < 100 \mu V$ for SHTE, AHTE or SM algorithms and manual assessment methods are presented in Table 6. In Fig. 14a and 14b, the MEP PTP amplitude distribution of 388 signals divided into two amplitude bands ($V_{pp} < 50 \mu V$ and $50 \mu V > V_{pp} < 100 \mu V$) is presented. Also, Fig. 14 shows the expected normal distribution curve of PTP MEP signal amplitudes for these two amplitude bands.

Furthermore, Table 3 and Fig. 15 present the PDI results for validation of the AHTE, SHTE, and SM algorithms regarding manual assessment in $V_{pp} < 50 \mu V$ and $50 \mu V > V_{pp} < 100 \mu V$ amplitude bands. The two-way ANOVA was conducted for PDI of MEP latency using manual assessment as a reference point. Obtained results of F-tests

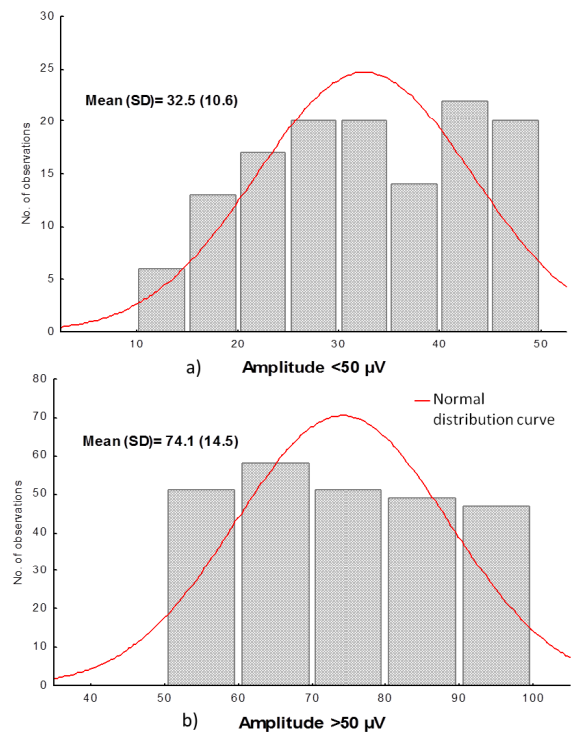


FIGURE 14. MEP PTP amplitude distribution of 388 signals for: a) $50 \mu V < V_{pp} < 100 \mu V$ amplitude band ($N_{V_{pp} < 50 \mu V} = 132$), b) $50 \mu V > V_{pp} < 100 \mu V$ amplitude band ($N_{50 \mu V > V_{pp} < 100 \mu V} = 256$).

and Fisher's LSD *post hoc* tests ($F_{\text{methods}} = 568.1, p < 0.001^*$; $F_{\text{amplitude}} = 22.6, p < 0.001^*$; $F_{\text{interaction}} = 12.1, p < 0.001^*$; *post hoc* SM-AHTE $_{[50-100]\mu V}, p < 0.001^*$; SM-SHTE $_{[50-100]\mu V}, p < 0.001^*$; AHTE-SHTE $_{>50\mu V},$

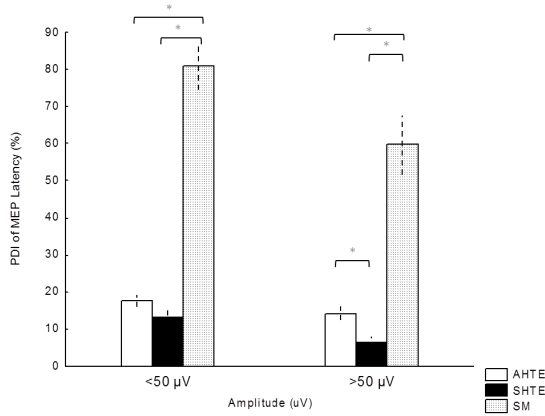


FIGURE 15. The percentage deviation of MEP latency estimation for SHTE, AHTE, and SM algorithms compared to manual assessment for the 388 MEP signals divided into two PTP amplitude bands ($V_{pp} < 50 \mu V$ and $50 \mu V > V_{pp} < 100 \mu V$).

$p < 0.001^*$; $AHTE-SM_{\epsilon[50-100]\mu V}$, $p < 0.001^*$; $SHTE-SM_{>50\mu V}$, $p < 0.001^*$) confirm the statistical difference of PDI mean values. Accordingly, SHTE has the lowest PDI mean values in amplitude range $V_{pp} < 50 \mu V$ and $50 \mu V > V_{pp} < 100 \mu V$ (Table 3).

Table 6 presents the NOH and robustness test results for MEP signal latency estimation of SHTE, AHTE, and SM algorithms in $V_{pp} < 50 \mu V$ and $50 \mu V > V_{pp} < 100 \mu V$ amplitude bands. According to Table 6, in the amplitude band $V_{pp} < 50 \mu V$, the SHTE algorithm performs robustly in AR1, AR2, AR4, and AR5, and less robustly in AR3. The AHTE algorithm performs robustly in AR2, AR3, and AR4, and less robustly in AR1 and AR5. Finally, the SM algorithm performs robustly in all ARs. For instance, in AR3, the SHTE, on average, scores $41.0 (\pm 0.9, SD)\%$ NOHs with the maximum and minimum values of 38.8% and 42.2% , respectively. This means the SHTE accurately estimates four out of ten MEP signal latencies in AR3 when the number of samples exceeds 40 MEP signals (see Table 7 in the Appendix). However, the AHTE and SM algorithms accurately estimate one out of ten MEP latencies in AR3, regardless of the sample size (Table 8 and Table 9 in the Appendix).

If the PTP amplitude band $50 \mu V > V_{pp} < 100 \mu V$ of analyzed MEP signals is observed, it can be seen that the SHTE algorithm performs robustly over all ARs, while the AHTE performs less robustly in AR3 and AR4 and the SM algorithm performs less robustly in AR4. On average, the SHTE algorithm accurately estimates seven out of ten MEP latencies in terms of NOH tests. Compared with AHTE and SM algorithms, accurate estimation is performed for four out of ten MEP latencies on average. Furthermore, the AHTE for the sample size of 26 samples (10% of 256 MEP signals, Table 11 in the Appendix) accurately estimates five out of ten MEP latencies.

Hence, the results presented in Table 6 confirm that the SHTE algorithm outperforms AHTE and SM algorithms in lower amplitude bands ($50 \mu V > V_{pp} < 100 \mu V$).

TABLE 7. Results of testing the robustness procedure for MEP signal latency estimation in amplitude band $V_{pp} < 50 \mu V$ for SHTE algorithm.

$V_{pp} < 50 \mu V$					
AR (Samples)	1	2	3	4	5
(Time res.)	(0.4 ms)	(0.7 ms)	(1.1 ms)	(1.5 ms)	(1.9 ms)
SHTE					
NOH/Sets (no. of MEP signals)	(%)	(%)	(%)	(%)	(%)
10% of 132 (14)	22.9	36.4	40.7	45.0	47.6
20% of 132 (27)	24.0	37.9	42.2	45.7	47.3
30% of 132 (40)	22.9	35.6	38.8	43.1	45.2
40% of 132 (53)	22.9	37.5	40.9	44.7	46.9
50% of 132 (66)	24.5	37.9	41.4	45.0	47.0
60% of 132 (80)	24.3	37.1	40.8	44.4	47.3
70% of 132 (93)	23.5	36.8	40.5	44.3	46.7
80% of 132 (106)	24.2	37.9	41.5	45.1	47.3
90% of 132 (119)	24.0	37.7	41.5	45.1	47.3
100% of 132 (132)	24.2	37.9	41.7	45.5	47.7
Min (%)	22.9	35.6	38.8	43.1	45.2
Max (%)	24.5	37.9	42.2	45.7	47.7
Average (%)	23.7	37.3	41.0	44.8	47.0
SD (%)	0.6	0.8	0.9	0.7	0.7

TABLE 8. Results of testing the robustness procedure for MEP Signal Latency estimation in amplitude band $V_{pp} < 50 \mu V$ for AHTE algorithm.

$V_{pp} < 50 \mu V$					
AR (Samples)	1	2	3	4	5
(Time res.)	(0.4 ms)	(0.7 ms)	(1.1 ms)	(1.5 ms)	(1.9 ms)
AHTE					
NOH/Sets (no. of MEP signals)	(%)	(%)	(%)	(%)	(%)
10% of 132 (14)	10.5	14.3	16.0	16.0	21.0
20% of 132 (27)	8.9	13.5	14.7	14.7	21.2
30% of 132 (40)	8.7	12.0	13.8	13.8	20.3
40% of 132 (53)	9.1	12.8	14.4	14.4	20.4
50% of 132 (66)	9.7	13.5	15.1	15.1	21.0
60% of 132 (80)	9.1	12.9	14.3	14.3	21.1
70% of 132 (93)	8.5	12.5	13.8	13.8	19.8
80% of 132 (106)	8.8	12.6	14.2	14.2	20.1
90% of 132 (119)	9.1	12.9	14.4	14.4	20.4
100% of 132 (132)	9.1	12.9	14.4	14.4	20.5
Min (%)	8.5	12.0	13.8	13.8	19.8
Max (%)	10.5	14.3	16.0	16.0	21.2
Average (%)	9.1	13.0	14.5	14.5	20.6
SD (%)	0.6	0.6	0.6	0.6	0.5

Finally, measuring the execution time for SHTE, AHTE, and SM algorithms result in the average execution time of 14.2 ms (11.2/15.3 ms, min./max), 21.1 ms (17.3/22.2 ms, min./max), and 17.6 ms (15.5/19.0 ms, min./max), respectively. This confirms the possibility of real practical implementation of the SHTE algorithm.

VII. DISCUSSION

It is to emphasize that performing a squaring operation on the MEPs coefficients brings the following benefit in using the SHTE algorithm. The SHTE and AHTE algorithms have the same procedure for determining the threshold value

TABLE 9. Results Of Testing The Robustness Procedure For MEP Signal Latency estimation in amplitude band $V_{pp} < 50 \mu V$ for SM algorithm.

$V_{pp} < 50 \mu V$					
AR (Samples)	1	2	3	4	5
(Time res.)	(0.4 ms)	(0.7 ms)	(1.1 ms)	(1.5 ms)	(1.9 ms)
SM					
NOH/ Sets (no. of MEP signals)	(%)	(%)	(%)	(%)	(%)
10% of 132 (14)	6.7	14.8	14.8	17.1	18.1
20% of 132 (27)	7.4	14.2	14.2	16.7	17.7
30% of 132 (40)	6.0	13.6	13.6	15.8	16.5
40% of 132 (53)	6.5	13.3	13.3	16.2	16.7
50% of 132 (66)	7.1	15.0	15.0	17.3	17.9
60% of 132 (80)	6.9	14.5	14.5	16.6	17.2
70% of 132 (93)	6.4	14.0	14.0	16.1	16.8
80% of 132 (106)	7.0	14.3	14.3	16.6	17.4
90% of 132 (119)	6.7	14.0	14.0	16.4	17.1
100% of 132 (132)	6.8	14.4	14.4	16.7	17.4
Min (%)	6.0	13.3	13.3	15.8	16.5
Max (%)	7.4	15.0	15.0	17.3	18.1
Average (%)	6.8	14.2	14.2	16.5	17.3
SD (%)	0.4	0.5	0.5	0.5	0.5

(i.e., finding 10% of V_{max} in the case of the AHTE (Figure 1) and finding 10% of X_{max} in the case of SHTE (Figure 6)). However, in the case of the SHTE, 10% of X_{max} transforms in 31.6% of V_{max} of the AHTE algorithm. When the threshold value is changed above 10% of V_{max} , this can produce more samples between the start of the MEP and the crossing threshold line. Since triggered MEP could have some local maximum(s) and/or minimum(s) between the starting point and V_{max} , the MEPs morphological structure could contribute to the estimation error. Hence, the morphological structure of the MEP plays an important role in determining the starting point. More samples mean that there are more points to shape potential local minimum(s) and maximum(s). Lowering the threshold value leads to the better determination of the magic number, but at the same time reduces the latency estimation accuracy of the MEP signals with amplitudes lower than $100 \mu V$ (due to so-called “muscle noise”). Also, by exploiting the same threshold calculation (equal to 10 % of the maximum amplitude of squared coefficients), the proposed algorithm ensures the same magic number as an important value in estimating the MEP latency signal. This contributes to the improvement of the algorithm execution performance and reliability.

In this study, we compared the SHTE algorithm with algorithms based on AHTE, the SM, and manual assessment as the reference. Obtained results show that the SHTE algorithm had similar achievements in the MEP latency estimation of all MEP signals on the entire amplitude bands level. When considering the MEP signal’s specific amplitude band, the differences in the assessment of MEP latency among the algorithms are observed. This is especially confirmed for the estimation of MEP signal latencies having amplitudes lower than $100 \mu V$. In this case, the SHTE algorithm outperforms AHTE and SM for MEP signal latency estimation. This is also

TABLE 10. Results of testing the robustness procedure for MEP signal latency estimation in amplitude band $50 \mu V > V_{pp} < 100 \mu V$ for SHTE algorithm.

$50 \mu V > V_{pp} < 100 \mu V$					
AR (Samples)	1	2	3	4	5
(Time res.)	(0.4 ms)	(0.7 ms)	(1.1 ms)	(1.5 ms)	(1.9 ms)
SHTE					
NOH/ Sets (no. of MEP signals)	(%)	(%)	(%)	(%)	(%)
10% of 256 (26)	44.0	66.8	77.1	79.7	82.7
20% of 256 (52)	41.7	62.0	73.8	77.9	82.8
30% of 256 (77)	43.2	63.5	74.2	78.7	82.8
40% of 256 (103)	43.0	63.0	74.5	78.8	83.0
50% of 256 (128)	43.0	64.1	75.1	79.6	84.0
60% of 256 (154)	42.4	62.9	74.0	78.4	82.7
70% of 256 (180)	42.9	62.9	74.1	78.6	82.8
80% of 256 (205)	42.3	62.7	74.1	78.4	82.7
90% of 256 (231)	42.7	63.1	74.6	78.8	83.0
100% of 256 (256)	42.6	62.9	74.2	78.5	82.8
Min (%)	41.7	62.0	73.8	77.9	82.7
Max (%)	44.0	66.8	77.1	79.7	84.0
Average (%)	42.8	63.4	74.6	78.8	82.9
SD (%)	0.6	1.3	1.0	0.5	0.4

TABLE 11. Results of testing the robustness procedure for MEP signal latency estimation in amplitude band $50 \mu V > V_{pp} < 100 \mu V$ for AHTE algorithm.

$50 \mu V > V_{pp} < 100 \mu V$					
AR (Samples)	1	2	3	4	5
(Time res.)	(0.4 ms)	(0.7 ms)	(1.1 ms)	(1.5 ms)	(1.9 ms)
AHTE					
NOH/ Sets (no. of MEP signals)	(%)	(%)	(%)	(%)	(%)
10% of 256 (26)	33.8	44.6	50.6	52.1	53.8
20% of 256 (52)	30.3	40.7	47.1	49.6	53.0
30% of 256 (77)	31.7	41.0	47.6	50.2	53.7
40% of 256 (103)	31.0	41.9	48.7	50.8	53.9
50% of 256 (128)	32.0	42.7	49.2	51.4	54.5
60% of 256 (154)	31.2	41.8	48.3	50.8	53.7
70% of 256 (180)	31.0	41.0	47.5	49.9	53.0
80% of 256 (205)	31.4	41.9	48.4	50.6	53.7
90% of 256 (231)	30.9	41.6	48.2	50.6	53.8
100% of 256 (256)	30.9	41.4	48.0	50.4	53.5
Min (%)	30.3	40.7	47.1	49.6	53.0
Max (%)	33.8	44.6	50.6	52.1	54.5
Average (%)	31.4	41.9	48.4	50.6	53.7
SD (%)	1.0	1.1	1.0	0.7	0.4

confirmed with the results obtained for the robustness test and NOH. The PDI results additionally prove the differences in validating methods for different MEP amplitude bands. Compared to other tested algorithms, SHTE has a lower PDI in estimating the MEP latency of the MEP signals with the PTP amplitudes lower than $100 \mu V$ ($V_{pp} < 100 \mu V$ and $50 \mu V > V_{pp} < 100 \mu V$). Hence, the obtained results confirm the possibility of implementing the proposed SHTE algorithm for clinical and research purposes.

To increase the chances to elicit a more robust sample of MEP responses, the approach used in this work was based on

TABLE 12. Results of testing the robustness procedure for MEP signal latency estimation in amplitude band $50 \mu\text{V} > V_{pp} < 100 \mu\text{V}$ for SM algorithm.

$50 \mu\text{V} > V_{pp} < 100 \mu\text{V}$					
AR (Samples)	1	2	3	4	5
(Time res.)	(0.4 ms)	(0.7 ms)	(1.1 ms)	(1.5 ms)	(1.9 ms)
SM					
NOH/ Sets (no. of MEP signals)	(%)	(%)	(%)	(%)	(%)
10% of 256 (26)	25.5	39.5	45.8	51.2	53.8
20% of 256 (52)	25.1	37.9	45.1	48.5	52.6
30% of 256 (77)	24.8	37.5	44.4	48.7	52.2
40% of 256 (103)	24.4	37.6	45.1	49.5	52.6
50% of 256 (128)	24.8	37.9	45.4	49.8	53.3
60% of 256 (154)	23.8	36.8	44.1	48.5	52.2
70% of 256 (180)	24.6	37.3	44.6	49.0	52.7
80% of 256 (205)	24.6	37.5	44.9	49.3	52.8
90% of 256 (231)	24.8	37.7	44.9	49.3	52.8
100% of 256 (256)	24.6	37.5	44.9	49.2	52.7
Min (%)	23.8	36.8	44.1	48.5	52.2
Max (%)	25.5	39.5	45.8	51.2	53.8
Average (%)	24.7	37.7	44.9	49.3	52.8
SD (%)	0.4	0.7	0.5	0.8	0.5

TABLE 13. Results of testing the robustness procedure for MEP signal latency estimation in amplitude band $V_{pp} < 100 \mu\text{V}$ For SHTE algorithm.

$V_{pp} < 100 \mu\text{V}$					
AR (Samples)	1	2	3	4	5
(Time res.)	(0.4 ms)	(0.7 ms)	(1.1 ms)	(1.5 ms)	(1.9 ms)
SHTE					
NOH/ Sets (no. of MEP signals)	(%)	(%)	(%)	(%)	(%)
10% of 388 (39)	36.5	54.4	63.8	67.1	70.2
20% of 388 (78)	37.8	54.8	64.7	68.9	72.6
30% of 388 (117)	36.8	54.6	63.2	67.2	70.9
40% of 388 (156)	36.6	54.4	63.1	67.3	70.9
50% of 388 (194)	35.9	54.6	63.5	67.8	71.2
60% of 388 (233)	36.2	54.3	62.9	67.1	70.9
70% of 388 (272)	36.3	54.2	63.1	67.1	70.7
80% of 388 (311)	36.6	54.3	63.2	67.3	70.8
90% of 388 (350)	36.4	54.4	63.3	67.4	70.9
100% of 388 (388)	36.3	54.4	63.1	67.3	70.9
Min (%)	35.9	54.2	62.9	67.1	70.2
Max (%)	37.8	54.8	64.7	68.9	72.6
Average (%)	36.5	54.4	63.4	67.5	71.0
SD (%)	0.5	0.2	0.5	0.6	0.6

exploiting the SAI protocol. Due to variable PTP MEP amplitudes, an SAI protocol approach offers higher opportunities to elicit suppression of MEP amplitudes. It is reasonable to believe that including 889 MEP signals from 19 different subjects offers adequate MEP variability for testing the SHTE algorithm and comparing it with other prominent algorithms. Presented statistical analyses showed that the sample size in each amplitude band was sufficient for comparing the latency estimation performance of the SHTE with other algorithms. The developed SHTE algorithm presented in this work contributes to the improvement of speed in obtaining the accurate

TABLE 14. Results of testing the robustness procedure for MEP signal latency estimation in amplitude band $V_{pp} < 100 \mu\text{V}$ for AHTE algorithm.

$V_{pp} < 100 \mu\text{V}$					
AR (Samples)	1	2	3	4	5
(Time res.)	(0.4 ms)	(0.7 ms)	(1.1 ms)	(1.5 ms)	(1.9 ms)
AHTE					
NOH/ Sets (no. of MEP signals)	(%)	(%)	(%)	(%)	(%)
10% of 388 (39)	22.1	31.6	35.8	38.0	42.1
20% of 388 (78)	23.2	32.1	36.7	38.6	42.5
30% of 388 (117)	24.5	32.5	37.0	38.8	42.7
40% of 388 (156)	23.5	31.6	36.6	38.1	42.4
50% of 388 (194)	23.5	31.9	36.6	37.9	42.1
60% of 388 (233)	22.8	31.0	35.9	37.3	41.3
70% of 388 (272)	23.3	31.6	36.4	37.8	42.1
80% of 388 (311)	23.4	31.8	36.5	38.0	42.2
90% of 388 (350)	23.7	31.9	36.9	38.4	42.4
100% of 388 (388)	23.5	31.7	36.6	38.1	42.3
Min (%)	22.1	31.0	35.8	37.3	41.3
Max (%)	24.5	32.5	37.0	38.8	42.7
Average (%)	23.4	31.8	36.5	38.1	42.2
SD (%)	0.6	0.4	0.4	0.4	0.4

TABLE 15. Results of testing the robustness procedure for latency estimation in amplitude band $V_{pp} < 100 \mu\text{V}$ for SM algorithm.

$V_{pp} < 100 \mu\text{V}$					
AR (Samples)	1	2	3	4	5
(Time res.)	(0.4 ms)	(0.7 ms)	(1.1 ms)	(1.5 ms)	(1.9 ms)
SM					
NOH/ Sets (no. of MEP signals)	(%)	(%)	(%)	(%)	(%)
10% of 388 (39)	19.1	28.2	32.1	36.2	38.6
20% of 388 (78)	17.9	30.6	35.3	38.9	41.9
30% of 388 (117)	18.1	30.4	34.9	38.5	41.2
40% of 388 (156)	18.4	30.5	35.4	39.0	41.5
50% of 388 (194)	18.3	29.7	34.9	38.6	40.9
60% of 388 (233)	17.9	29.2	33.9	37.3	39.7
70% of 388 (272)	18.1	29.3	34.2	37.8	40.3
80% of 388 (311)	18.6	29.6	34.6	38.1	40.7
90% of 388 (350)	18.6	29.6	34.6	38.3	40.8
100% of 388 (388)	18.6	29.6	34.5	38.1	40.7
Min (%)	17.9	28.2	32.1	36.2	38.6
Max (%)	19.1	30.6	35.4	39.0	41.9
Average (%)	18.4	29.7	34.4	38.1	40.6
SD (%)	0.4	0.7	1.0	0.8	0.9

estimation of MEP latency, especially for MEP signals with low-amplitudes ($V_{pp} < 100 \mu\text{V}$). The execution time of the SHTE algorithm is similar to other tested algorithms (AHTE, SM) since the SHTE algorithm comprises an almost equal number of execution steps (phases), differing in square operation, which is not computationally demanding.

Finally, the following limitation of the study has to be pointed out. The parameter T_{DZ} (defined as the duration of the dropout zone time), which has to be set at the beginning of the study, was embedded in SHTE and AHTE algorithms. In our study, the T_{DZ} was set to 18 ms, which was determined by the MEP latency norms for APB and FDI hand muscles [2].

TABLE 16. Results on testing the robustness procedure for MEP latency estimation in amplitude band $V_{pp} > 100 \mu V$ for SHTE algorithm.

$V_{pp} > 100 \mu V$					
AR (Samples) (Time res.)	1 (0.4ms)	2 (0.7 ms)	3 (1.1ms)	4 (1.5ms)	5 (1.9ms)
SHTE					
NOH/ Sets (no. of MEP signals)	(%)	(%)	(%)	(%)	(%)
10% of 501 (51)	64.4	79.7	88.4	94.8	96.8
20% of 501 (102)	64.6	79.9	89.1	95.7	97.9
30% of 501 (151)	63.8	79.7	88.5	95.6	97.5
40% of 501 (201)	64.1	79.6	88.6	95.6	97.6
50% of 501 (251)	64.4	79.5	88.1	95.3	97.4
60% of 501 (301)	63.6	79.0	88.0	95.7	97.8
70% of 501 (351)	64.3	79.4	88.4	95.5	97.6
80% of 501 (401)	64.2	79.6	88.3	95.7	97.6
90% of 501 (451)	64.1	79.3	88.1	95.5	97.6
100% of 501 (501)	64.3	79.4	88.2	95.6	97.6
Min (%)	63.6	79.0	88.0	94.8	96.8
Max (%)	64.6	79.9	89.1	95.7	97.9
Average (%)	64.2	79.5	88.4	95.5	97.5
SD (%)	0.3	0.2	0.3	0.3	0.3

TABLE 17. Results of testing the robustness procedure for MEP latency estimation in amplitude band $V_{pp} > 100 \mu V$ for AHTE algorithm.

$V_{pp} > 100 \mu V$					
AR (Samples) (Time res.)	1 (0.4 ms)	2 (0.7 ms)	3 (1.1 ms)	4 (1.5 ms)	5 (1.9 ms)
AHTE					
NOH/ Sets (no. of MEP signals)	(%)	(%)	(%)	(%)	(%)
10% of 501 (51)	69.0	82.9	89.0	93.8	95.4
20% of 501 (102)	70.3	83.5	89.4	93.9	95.5
30% of 501 (151)	70.2	83.6	89.2	94.2	95.7
40% of 501 (201)	70.6	84.1	90.3	94.5	96.0
50% of 501 (251)	70.2	83.7	90.2	94.8	96.2
60% of 501 (301)	69.2	83.5	89.9	94.6	95.9
70% of 501 (351)	70.5	84.0	90.0	94.6	96.1
80% of 501 (401)	70.0	83.9	90.1	94.6	96.1
90% of 501 (451)	70.1	83.9	90.1	94.7	96.1
100% of 501 (501)	70.1	83.8	90.0	94.6	96.0
Min (%)	69.0	82.9	89.0	93.8	95.4
Max (%)	70.6	84.1	90.3	94.8	96.2
Average (%)	70.0	83.7	89.8	94.4	95.9
SD (%)	0.5	0.3	0.4	0.3	0.3

To fully investigate the applicability of the SHTE algorithm in the detection of latency of MEP signals with lower PTP amplitudes ($V_{pp} < 100 \mu V$), the proposed SHTE algorithm can be exploited in future nTMS studies on healthy subjects or patients having a tumour, spinal cord injury, neurology diseases, etc., using different protocols (i.e. resting and voluntary state, MEP recruitment curve, or other neurophysiological protocols).

VIII. CONCLUSION

In this article, the new SHTE algorithm for estimating MEP signal latency on the pattern of MEP signals collected from real subjects has been presented. The analysis was performed

TABLE 18. Results on testing the robustness procedure for MEP latency estimation in amplitude band $V_{pp} > 100 \mu V$ for SM algorithm.

$V_{pp} > 100 \mu V$					
AR (Samples) (Time res.)	1 (0.4ms)	2 (0.7 ms)	3 (1.1ms)	4 (1.5ms)	5 (1.9ms)
SM					
NOH/ Sets (no. of MEP signals)	(%)	(%)	(%)	(%)	(%)
10% of 501 (51)	55.5	78.6	85.5	92.9	96.3
20% of 501 (102)	54.2	78.9	86.0	92.7	97.0
30% of 501 (151)	54.2	78.2	85.5	92.0	96.6
40% of 501 (201)	54.3	79.2	86.1	92.9	97.0
50% of 501 (251)	53.7	78.5	85.5	92.5	96.8
60% of 501 (301)	53.8	78.5	85.3	92.8	97.0
70% of 501 (351)	54.4	78.8	85.5	92.6	96.8
80% of 501 (401)	54.5	79.0	85.8	92.8	96.9
90% of 501 (451)	54.2	78.8	85.6	92.5	96.8
100% of 501 (501)	54.1	78.8	85.6	92.6	96.8
Min (%)	53.7	78.2	85.3	92.0	96.3
Max (%)	55.5	79.2	86.1	92.9	97.0
Average (%)	54.3	78.7	85.6	92.6	96.8
SD (%)	0.5	0.3	0.2	0.3	0.2

on the large number of MEP signals acquired with the nTMS approach from subjects in resting-state, engaged in SAI protocol. The validation of the SHTE algorithm was conducted by comparing the latency estimation efficiency of the proposed SHTE algorithm with prominent algorithms based on AHTE and the SM while taking the manual assessment of MEP signals as the reference validation.

Obtained results for the robustness test show the evident advantage of using the SHTE algorithm in automatic MEP latency estimation in all amplitude bands. Also, results related to PDI proved that SHTE in comparison to AHTE and SM algorithms has a lower PDI in estimating the MEP latency for the MEP signals with the PTP amplitudes lower than $100 \mu V$ ($V_{pp} < 100 \mu V$ and $50 \mu V > V_{pp} < 100 \mu V$). Hence, the results of analyses presented in this article confirm the possibility of implementing the SHTE algorithm in practical applications such as TMS research and medical clinic work.

The developed SHTE algorithm represents an improved armamentarium in MEP latency estimation for subjects in resting-state and can be tested for implementation with other neurophysiological states (i.e., voluntary state) and protocols (i.e., MEP recruitment curve). Moreover, performed comparison of the proposed SHTE algorithm with other algorithms in terms of efficiency in MEP latency estimation may contribute to understanding the factors underlying MEP latency variability, especially those demonstrated in the field of neurosurgery.

A future research activity will be focused on finding an optimal magic number for every MEP signal when the SHTE runs and thus improving NOHs in all amplitude bands (primary for MEP signals with PTP amplitudes lower than $100 \mu V$).

APPENDIX

See Tables 7–18.

ACKNOWLEDGMENT

The study was approved by the Ethics Committee of the School of Medicine, University of Split. All performed procedures were in accordance with the ethical standards of the institutional research committee and with 1964 Helsinki declaration and its later amendments. Informed consent was obtained from all subjects participating in tests.

REFERENCES

- [1] A. T. Barker, R. Jalinous, and I. L. Freeston, "NON-INVASIVE MAGNETIC STIMULATION OF HUMAN MOTOR CORTEX," *Lancet*, vol. 325, no. 8437, pp. 1106–1107, May 1985.
- [2] P. M. Rossini, "Non-invasive electrical and magnetic stimulation of the brain, spinal cord, roots and peripheral nerves: Basic principles and procedures for routine clinical and research application. An updated report from an I.F.C.N. Committee," *Clin. Neurophysiol.*, vol. 126, no. 6, pp. 1071–1107, Jun. 2015, doi: [10.1016/j.clinph.2015.02.001](https://doi.org/10.1016/j.clinph.2015.02.001).
- [3] T. Krings, B. R. Buchbinder, W. E. Butler, and K. H. Chiappa, "Stereotactic transcranial magnetic stimulation: Correlation with direct electrical cortical stimulation," *Neurosurgery*, vol. 41, no. 6, pp. 1319–1325, Dec. 1997, doi: [10.1097/00006123-199712000-00016](https://doi.org/10.1097/00006123-199712000-00016).
- [4] T. Krings, B. R. Buchbinder, W. E. Butler, K. H. Chiappa, H. J. Jiang, G. R. Cosgrove, and B. R. Rosen, "Functional magnetic resonance imaging and transcranial magnetic stimulation: Complementary approaches in the evaluation of cortical motor function," *Neurology*, vol. 48, no. 5, pp. 1406–1416, May 1997, doi: [10.1212/wnl.48.5.1406](https://doi.org/10.1212/wnl.48.5.1406).
- [5] T. Picht, J. Schulz, and P. Vajkoczy, "The preoperative use of navigated transcranial magnetic stimulation facilitates early resection of suspected low-grade gliomas in the motor cortex," *Acta Neurochirurgica*, vol. 155, no. 10, pp. 1813–1821, Oct. 2013, doi: [10.1007/s00701-013-1839-1](https://doi.org/10.1007/s00701-013-1839-1).
- [6] T. Picht, D. Frey, S. Thieme, S. Kliesch, and P. Vajkoczy, "Presurgical navigated TMS motor cortex mapping improves outcome in glioblastoma surgery: A controlled observational study," *J. Neuro-Oncol.*, vol. 126, no. 3, pp. 535–543, Feb. 2016, doi: [10.1007/s11060-015-1993-9](https://doi.org/10.1007/s11060-015-1993-9).
- [7] P. E. Tarapore, T. Picht, L. Bulubas, Y. Shin, N. Kulchytka, B. Meyer, M. S. Berger, S. S. Nagarajan, and S. M. Krieg, "Safety and tolerability of navigated TMS for preoperative mapping in neurosurgical patients," *Clin. Neurophysiol.*, vol. 127, no. 3, pp. 1895–1900, Mar. 2016, doi: [10.1016/j.clinph.2015.11.042](https://doi.org/10.1016/j.clinph.2015.11.042).
- [8] A.-M. Vitikainen, P. Lioumis, R. Paetau, E. Salli, S. Komssi, L. Metsähonkala, A. Paetau, D. Kičić, G. Blomstedt, L. Valanne, J. P. Mäkelä, and E. Gaily, "Combined use of non-invasive techniques for improved functional localization for a selected group of epilepsy surgery candidates," *NeuroImage*, vol. 45, no. 2, pp. 342–348, Apr. 2009, doi: [10.1016/j.neuroimage.2008.12.026](https://doi.org/10.1016/j.neuroimage.2008.12.026).
- [9] J. P. Mäkelä, A.-M. Vitikainen, P. Lioumis, R. Paetau, E. Ahtola, L. Kuusela, L. Valanne, G. Blomstedt, and E. Gaily, "Functional plasticity of the motor cortical structures demonstrated by navigated TMS in two patients with epilepsy," *Brain Stimulation*, vol. 6, no. 3, pp. 286–291, May 2013, doi: [10.1016/j.brs.2012.04.012](https://doi.org/10.1016/j.brs.2012.04.012).
- [10] L. Säisänen, M. Könönen, P. Julkunen, S. Määttä, R. Vanninen, A. Immonen, L. Jutila, R. Kälviäinen, J. E. Jääskeläinen, and E. Mervaala, "Non-invasive preoperative localization of primary motor cortex in epilepsy surgery by navigated transcranial magnetic stimulation," *Epilepsy Res.*, vol. 92, nos. 2–3, pp. 134–144, Dec. 2010, doi: [10.1016/j.eplepsyres.2010.08.013](https://doi.org/10.1016/j.eplepsyres.2010.08.013).
- [11] S. Schmidt, E. Holst, K. Irlbacher, F. Oltmanns, M. Merschhemke, and S. A. Brandt, "A case of pathological excitability located with navigated-TMS: Presurgical evaluation of focal neocortical epilepsy," *Restorative Neurol. Neurosci.*, vol. 28, no. 3, pp. 379–385, 2010, doi: [10.3233/RNN-2010-0540](https://doi.org/10.3233/RNN-2010-0540).
- [12] A.-M. Vitikainen, E. Salli, P. Lioumis, J. P. Mäkelä, and L. Metsähonkala, "Applicability of nTMS in locating the motor cortical representation areas in patients with epilepsy," *Acta Neurochirurgica*, vol. 155, no. 3, pp. 507–518, Mar. 2013, doi: [10.1007/s00701-012-1609-5](https://doi.org/10.1007/s00701-012-1609-5).
- [13] A. Conti, A. Pontoriero, G. K. Ricciardi, F. Granata, S. Vinci, F. F. Angileri, S. Pergolizzi, C. Alafaci, V. Rizzo, A. Quartarone, A. Germañ, R. I. Foroni, C. De Renzi, and F. Tomasello, "Integration of functional neuroimaging in CyberKnife radiosurgery: Feasibility and dosimetric results," *Neurosurgical Focus*, vol. 34, no. 4, p. E5, Apr. 2013, doi: [10.3171/2013.2.FOCUS12414](https://doi.org/10.3171/2013.2.FOCUS12414).
- [14] N. Kato, S. Schilt, H. Schneider, D. Frey, M. Kufeld, P. Vajkoczy, and T. Picht, "Functional brain mapping of patients with arteriovenous malformations using navigated transcranial magnetic stimulation: First experience in ten patients," *Acta Neurochirurgica*, vol. 156, no. 5, pp. 885–895, May 2014, doi: [10.1007/s00701-014-2043-7](https://doi.org/10.1007/s00701-014-2043-7).
- [15] J. C. Rothwell, "Magnetic stimulation: Motor evoked potentials," *Electroencephalogr. Clin. Neurophysiol.*, vol. 52, pp. 97–103, 1999.
- [16] V. Di Lazzaro, "The physiological basis of transcranial motor cortex stimulation in conscious humans," *Clin. Neurophysiol.*, vol. 115, no. 2, pp. 255–266, Feb. 2004, doi: [10.1016/j.clinph.2003.10.009](https://doi.org/10.1016/j.clinph.2003.10.009).
- [17] S. Bestmann and J. W. Krakauer, "The uses and interpretations of the motor-evoked potential for understanding behaviour," *Exp. Brain Res.*, vol. 233, no. 3, pp. 679–689, Mar. 2015, doi: [10.1007/s00221-014-4183-7](https://doi.org/10.1007/s00221-014-4183-7).
- [18] N. Sollmann, L. Bulubas, N. Tanigawa, C. Zimmer, B. Meyer, and S. M. Krieg, "The variability of motor evoked potential latencies in neurosurgical motor mapping by preoperative navigated transcranial magnetic stimulation," *BMC Neurosci.*, vol. 18, no. 1, Dec. 2017, doi: [10.1186/s12868-016-0321-4](https://doi.org/10.1186/s12868-016-0321-4).
- [19] D. T. A. Nguyen, S. M. Rissanen, P. Julkunen, E. Kallioniemi, and P. A. Karjalainen, "Principal component regression on motor evoked potential in single-pulse transcranial magnetic stimulation," *IEEE Trans. Neural Syst. Rehabil. Eng.*, vol. 27, no. 8, pp. 1521–1528, Aug. 2019.
- [20] L. Kiers, D. Cros, K. H. Chiappa, and J. Fang, "Variability of motor potentials evoked by transcranial magnetic stimulation," *Electroencephalogr. Clin. Neurophysiol./Evoked Potentials Sect.*, vol. 89, no. 6, pp. 415–423, Dec. 1993, doi: [10.1016/0168-5597\(93\)90115-6](https://doi.org/10.1016/0168-5597(93)90115-6).
- [21] L. Säisänen, P. Julkunen, E. Niskanen, N. Danner, T. Hukkanen, T. Lohioja, J. Nurkkala, E. Mervaala, J. Karhu, and M. Könönen, "Motor potentials evoked by navigated transcranial magnetic stimulation in healthy subjects," *J. Clin. Neurophysiol.*, vol. 25, no. 6, pp. 367–372, Dec. 2008, doi: [10.1097/WNP.0b013e31818e7944](https://doi.org/10.1097/WNP.0b013e31818e7944).
- [22] E. M. Wassermann, "Variation in the response to transcranial magnetic brain stimulation in the general population," *Clin Neurophysiol.*, vol. 113, no. 7, pp. 1165–1171, Jul. 2002, doi: [10.1016/s1388-2457\(02\)00144-x](https://doi.org/10.1016/s1388-2457(02)00144-x).
- [23] S. Ratnadurai Giridharan, D. Gupta, A. Pal, A. M. Mishra, N. J. Hill, and J. B. Carmel, "Motometrics: A toolbox for annotation and efficient analysis of motor evoked potentials," *Frontiers Neuroinform.*, vol. 13, Mar. 2019, doi: [10.3389/fninf.2019.00008](https://doi.org/10.3389/fninf.2019.00008).
- [24] S. Harquel, "CortExTool: A toolbox for processing motor cortical excitability measurements by transcranial magnetic stimulation," CNRS, UMR 5105, Laboratoire de Psychologie et de NeuroCognition, Grenoble, France, Tech. Rep. hal-01390016, 2016.
- [25] S. Harquel, "Robotized Transcranial Magnetic Stimulation: from automated protocols towards new approaches in functional neuroimaging," Ph.D. dissertation, Grenoble Inst. des Neurosci., Laboratoire de Psychologie et NeuroCognition, Neurosci., Univ. Grenoble-Alpes, Grenoble, France, 2017.
- [26] *MEPHunter, a Free Software for Signal Visualization and Analysis*, NeuroMat, Paulo, Brazil, 2014.
- [27] T. Picht, V. Strack, J. Schulz, A. Zdunczyk, D. Frey, S. Schmidt, and P. Vajkoczy, "Assessing the functional status of the motor system in brain tumor patients using transcranial magnetic stimulation," *Acta Neurochirurgica*, vol. 154, no. 11, pp. 2075–2081, Nov. 2012, doi: [10.1007/s00701-012-1494-y](https://doi.org/10.1007/s00701-012-1494-y).
- [28] S. Tremblay, "Clinical utility and prospective of TMS-EEG," *Clin. Neurophysiol.*, vol. 130, no. 5, pp. 802–844, May 2019, doi: [10.1016/j.clinph.2019.01.001](https://doi.org/10.1016/j.clinph.2019.01.001).
- [29] N. J. Davey, H. C. Smith, E. Wells, D. W. Maskill, G. Savic, P. H. Ellaway, and H. L. Frankel, "Responses of thenar muscles to transcranial magnetic stimulation of the motor cortex in patients with incomplete spinal cord injury," *J. Neurol., Neurosurg. Psychiatry*, vol. 65, no. 1, pp. 80–87, Jul. 1998, doi: [10.1136/jnnp.65.1.80](https://doi.org/10.1136/jnnp.65.1.80).
- [30] T. Tsuji and J. C. Rothwell, "Long lasting effects of rTMS and associated peripheral sensory input on MEPs, SEPs and transcortical reflex excitability in humans," *J. Physiol.*, vol. 540, no. 1, pp. 367–376, Apr. 2002, doi: [10.1113/jphysiol.2001.013504](https://doi.org/10.1113/jphysiol.2001.013504).
- [31] M. R. Vidaković, J. Šoda, A. Jerković, B. Benzon, K. Bakrač, S. Dužević, I. Vujović, M. Mihalj, R. Pecotić, M. Valić, A. Mastelić, M. V. Hagelien, M. Z. Schonwald, and Z. Dogas, "Obstructive sleep apnea syndrome: A preliminary navigated transcranial magnetic stimulation study," *Nature Sci. Sleep*, vol. Volume 12, pp. 563–574, Aug. 2020, doi: [10.2147/NSS.S253281](https://doi.org/10.2147/NSS.S253281).

- [32] R. C. Oldfield, "The assessment and analysis of handedness: The Edinburgh inventory," *Neuropsychologia*, vol. 9, no. 1, pp. 97–113, 1971, doi: [10.1016/0028-3932\(71\)90067-4](https://doi.org/10.1016/0028-3932(71)90067-4).
- [33] J. Ruohonen and J. Karhu, "Navigated transcranial magnetic stimulation," *Neurophysiologie Clinique/Clin. Neurophysiol.*, vol. 40, no. 1, pp. 7–17, Mar. 2010, doi: [10.1016/j.neucli.2010.01.006](https://doi.org/10.1016/j.neucli.2010.01.006).
- [34] S. M. Krieg, P. Lioumis, J. P. Mäkelä, J. Wilenius, J. Karhu, H. Hannula, P. Savolainen, C. W. Lucas, K. Seidel, A. Laakso, M. Islam, S. Vaalto, H. Lehtinen, A.-M. Vitikainen, P. E. Tarapore, and T. Picht, "Protocol for motor and language mapping by navigated TMS in patients and healthy volunteers; workshop report," *Acta Neurochirurgica*, vol. 159, no. 7, pp. 1187–1195, Jul. 2017, doi: [10.1007/s00701-017-3187-z](https://doi.org/10.1007/s00701-017-3187-z).
- [35] H. Tokimura, V. Di Lazzaro, Y. Tokimura, A. Oliviero, P. Profice, A. Insola, P. Mazzone, P. Tonali, and J. C. Rothwell, "Short latency inhibition of human hand motor cortex by somatosensory input from the hand," *J. Physiol.*, vol. 523, no. 2, pp. 503–513, Mar. 2000, doi: [10.1111/j.1469-7793.2000.t01-1-00503.x](https://doi.org/10.1111/j.1469-7793.2000.t01-1-00503.x).



JOŠKO ŠODA (Member, IEEE) received the B.S., M.S., and Ph.D. degrees in electrical engineering from the Faculty of Electrical Engineering, Mechanical Engineering, and Naval Architecture (FESB), University of Split, in 1999, 2005, and 2010, respectively. From 2001 to 2012, he has worked as a Research Assistant with the Department of Electronics and Computing, FESB. Since 2012, he has been working with the Faculty of Maritime Studies, University of Split, where he

currently holds the position of an Associate Professor. He has participated in eight research projects funded by the private or public sector. He has authored more than 30 scientific papers published in different scientific conferences and journals. His research interests include time-frequency analysis, learning and classification algorithms, statistical signal processing, applied signal processing in medicine, and the Internet of Things (IoT) in the industry. He is an EASE and an IEEE member of Signal Processing and Computer societies.



MAJA ROGIĆ VIDAKOVIĆ was born in Zadar, Croatia, in December 1982. She received the Master of Speech and Language Pathology (MSLP) degree from the Faculty of Education and Rehabilitation Sciences, University of Zagreb, in 2005, the Master of Science (M.Sc.) degree in neuroscience from the Graduate School of Neural and Behavioural Sciences, International Max Planck Research School, Eberhard Karls University, Tübingen, Germany, in 2008, and the Ph.D.

degree in neuroscience from the University of Split, Croatia, in 2012. From 2009 to 2012, she was a Research Fellow and, from 2012 to 2020, the Research Fellow—a Senior Research Assistant with the School of Medicine, University of Split. Since 2020, she has been the Research Associate with the Department of Neuroscience, School of Medicine, University of Split. Since 2013, she has been the Head of the Laboratory for Human and Experimental Neurophysiology (LAHEN), Department of Neuroscience, School of Medicine, Split, Croatia. She is the author of more than 20 scientific papers published in different scientific conferences and journals. Her research interests include preoperative mappings of higher cognitive functions, TMS, and simulation methodologies for mapping eloquent brain areas. Her current research interests include the application of TMS in the research of biomarkers in depression, multiple sclerosis, the introduction of TMS-EEG in the studies, and the development of algorithms for the analysis of MEP signals. She is a member of the Clinical TMS Society, the Croatian Society for Neuroscience, the Croatian Logopedic Association, the Croatian Dyslexia Association, and the Croatian Federation for EEG and Clinical Neurophysiology of the Croatian Medical Association. She holds two awards for the 1st–Best Poster Award at the International Symposium on Navigated Brain Stimulation in Neurosurgery and Neuromodulation, Berlin, Germany, in 2012 and 2015. She is the Topic Editor and an Associate Editor for the *Frontiers in Human Neuroscience* journal.



JOSIP LORINCZ (Senior Member, IEEE) received the B.Sc. (M.S. equivalent) and Ph.D. degrees in telecommunications engineering and computer science from the Faculty of Electrical Engineering, Mechanical Engineering, and Naval Architecture (FESB), University of Split, Croatia, in 2002 and 2010, respectively. In 2003, he joined the Department of Electronics and Computing, FESB, University of Split, where he currently works as an Associate Professor. In the

2009/2010 academic year, he was a Visiting Researcher with the Advanced Network Technologies Laboratory, Politecnico di Milano, Milan, Italy. As the Project Leader or a Researcher, he has participated in more than 20 scientific and professional projects funded by the public or private sector. He has authored more than 40 research papers published in different scientific conferences and journals. His current research interests include energy-efficient wireless and wired networks, optimization in telecommunications, advanced design, the management and analyses of heterogeneous computer networks, and the performance evolution of routing protocols. He is a Senior Member of ACM and the First President of the Croatian ACM Chapter. He also serves as the Technical Program Committee Member of many international scientific conferences and a Reviewer of top scientific journals. Since 2004, he has owned the Cisco CCNA, CCAI, and BCMSN Certificates. He was awarded as the Outstanding Young Researcher by the Croatian Academy of Engineering in 2013. He is also the Founder and the Co-Chair of the Symposium on Green Networking and Computing, organized in the International Conference on Software, Telecommunications and Computer Networks (SoftCOM) frame.



ANA JERKOVIĆ was born in Split, Croatia, in November 1984. She received the master's degree in psychology from the Department of Psychology, University of Zadar, Croatia, in 2008. From 2008 to 2009, she was a Junior Assistant with the Department of Psychology, Faculty of Philosophy, University of Mostar, Bosnia, and Herzegovina (BIH). Since 2009, she has been working as a School Psychologist with the Primary School Petar Berislavić, Trogir, Croatia. From

2004 to 2006, she was a member of the organizational committee: Psychology days in Zadar, Department of Psychology, University of Zadar. In 2005, she was a member of the organization committee: 7th Alps Adria Conference in Psychology, Department of Psychology, University of Zadar. From 2010 to 2011, she has coordinated TIMSS and PIRLS projects in Primary School Dr. Jure Turić, Gospić, Croatia, The Trends in International Mathematics and Science Study and The Progress in International Reading Literacy Study. She is the author of six scientific articles, one book chapter, and three textbooks in education and neuropsychology.



IGOR VUJIĆ (Member, IEEE) received the B.Sc., M.S., and Ph.D. degrees in electrical engineering from the Faculty of Electrical Engineering, Mechanical Engineering and Naval Architecture (FESB), University of Split, Croatia, in 1997, 2004, and 2011, respectively.

He was an Assistant, a Lecturer, a Senior Lecturer, and an Assistant Professor with the Faculty of Maritime Studies, University of Split, where he is currently an Associate Professor. He is also the Head of Ph.D. study, the Leader of the Scientific Group New Technologies in Maritime, the Head of the Signal Processing, Analysis and Advanced Diagnostics Research and Education Laboratory (SPAADREL), and the Project Manager. He has authored more than 100 research papers published in different books, scientific conferences, and journals. His current research interests include signal processing, materials in electrical engineering, and new technologies. He is a member of EASE. He is also the Editor-in-Chief of ToMS.

...